Rock-slope failures in Norway; type, geometry, deformation mechanisms and stability

Alvar Braathen*, Lars Harald Blikra, Silje S. Berg & Frode Karlsen

Braathen, A., Blikra, L.H., Berg, S.S. & Karlsen, F.: Rock-slope failures in Norway; type, geometry and hazard. *Norwegian Journal of Geology*, Vol. 84, pp. 67-88. Trondheim 2004. ISSN 029-196X.

Extensive studies of Norwegian rock-slope failure areas support a subdivision into three principle types: (1) Rockfall areas, (2) rockslide areas, and (3) complex fields. The classification is based on structural geometry and style of deformation, slope gradient, and the volumes involved. Rockfall areas, or toppling sites, are found in sub-vertical mountain sides. One or more unstable blocks are bound by a steep crevasse near the slope edge that is nearly cliff-parallel, whereas cliff-oblique extension fractures limit the blocks laterally. Rockslide areas are found on moderately dipping slopes, where slope-parallel, basal sliding planes, or detachments (along foliation, exfoliation surfaces), bound unstable blocks. The block size is controlled by steep fractures. Complex fields reveal complicated structural geometries and a rough morphology. Typical structures include a back-bounding graben, trenches and local depressions, fault scarps, crevasses, rotated fault blocks and deep-seated, low-angle detachments. They also involve significantly larger rock volumes (> 10 mill m^3) than the other types. Complex fields can be subdivided into either listric or planar styles based on their internal fault geometry.

Several structural features are diagnostic for areas undergoing rock-slope deformation above a basal detachment. On a large scale, the areas consist of detached blocks resting on a low-angle fault (rock on rock) or fault-rock layer (membrane) above non-deformed bedrock. Fault rocks appear to be common. This is consistent with a two-layer model, with an upper layer of more or less fractured bedrock, and a lower detachment layer of non-cohesive fault rocks that have mechanical properties more like soil (soft sediments). Development of non-cohesive fault breccia and gouge along a basal detachment, and especially if altered to clay, may drastically reduce the stability of a rock-failure area.

Driving forces and deformation mechanisms in rock-slope failure areas can be evaluated from short-term factors, such as seismic activity, water pressure and/or frost-related processes. In addition, an important long-term factor is gradual change in mechanical properties of slide planes. High water pressure and/or frost wedging are presumably most important for present day rockfall areas. Gradual reduction in the shear resistance of a detachment layer in combination with water pressure and freeze-thaw processes are probably critical aspects of rockslide areas and complex fields. Seismic activity above a critical surface acceleration could cause the final triggering leading to an avalanche for all types of rock-slope failures.

*Alvar Braathen, Lars Harald Blikra; Geological Survey of Norway/International Centre of Geohazards, 7491 Trondheim, Norway; Silje S. Berg, Department of Earth Science, University of Bergen, Norway; Frode Karlsen; Statoil, Harstad, Norway. * Corresponding author: Alvar.Braathen@cipr.uib.no, now at Centre of Integrated Petroleum Research, University of Bergen, Norway.*

Introduction

Norwegian rock avalanches have had fatal consequences in historical times and more are statistically expected in the near future. In order to predict such events, there is obviously a need for a better understanding of rock-slope failures. Areas subjected to slope deformation can provide important insights into the actual cause of rock avalanching, and may help to identify key observations that warn or are precursors of future events. Some attention was focused on the stability of Norwegian rock slopes after the destructive rock-avalanches and tsunamis in Tafjord and Loen in 1934 and 1936. Especially important was the review of Bjerrum & Jørstad (1968) who addressed the general factors of importance for understanding the behaviour of rock slopes in Norway. The present study follows this line. It focuses in more detail on source areas for potential rock avalanches, using for the topic techniques and knowledge from structural geology.

Bouldery rock-avalanche deposits are common in most regions of Norway, as is documented by the number of mountain slopes and ridges that have collapsed in prehistorical times. As one would expect, these features are found in mountainous regions with steep valley sides, and are especially clear in the counties of Troms, Møre & Romsdal, and Sogn & Fjordane (e.g., Blikra et al. 2002; Blikra et al., in press). Distinctive for these regions are concentrations of rock-avalanche deposits in certain areas, indicating common causes, such as (i) weak rocks, (ii) steep cliff-faces, and/or (iii) earthquakes (e.g., Blikra et al. in press). The timing is critical when hazard evaluations are discussed. For example, a large earthquake would create widespread, synchronous avalanches. In contrast, at many places, rock avalanches can be shown to be repetitive, as seen on the bottom of several fjords, where a series of bouldery fans or lobes build thick packages (Blikra et al. 1999; 2002; in press). Onshore, timing can be constrained by, for example, dating organic material below rock-avalanche

deposits (e.g., Blikra et al. in press). However, good sites are hard to find, and much work remains to be done before one with certainty can claim that regional patterns reflect either a temporal series, or widespread, single events (earthquakes).

We define rock avalanches as gravitational mass movements involving a large mass of rock debris that slides, flows, or falls rapidly down a mountain slope, in accordance with Keller (1992) and Hungr et al. (2001). Other terms, e.g., rockslides and "sturtzstrom" (e.g., Eisbacher 1979; Hutchinson 1988) have also been applied. Rock avalanches are caused by instabilities in mountain slopes that are triggered by various local forces. Hence, the cause for an avalanche is to be found in the source area. There, in or on top of mountain sides, distinct structural patterns can be observed. Our aim is to identify such pre-avalanche deformation patterns and discuss their links to the driving forces. This type of deformation has earlier been referred to as 'depth creep' (Ter-Stepanian 1966), 'deep-seated creep' (Nemcok 1972), 'deep-seated continuous creep' (Hutchinson 1968), 'sackung' (Zischinky 1966; Varnes et al. 1989), 'gleitung' (Zischinky 1966), and 'mass rock creep' (Radbruch-Hall 1978; Chigira 1992; Chigira & Kiho 1994). We use the broad expression *pre-avalanche deformation* based on geometrical observations, since the term creep as commonly used reflects a slow deformation mechanism.

We apply the following definitions to our descriptions: (i) *Joint* is a fracture mode with a wall-normal opening that, when open, is a crevasse. (ii) *Shear fracture* is a structure with displacement parallel to the fracture walls, and is termed a *fault* when displacement exceeds 1 m. (iii) For simplicity, we use *extension fracture* for hybrid fractures, which are characterised by a combination of two or more of the other fracture modes. In addition, we use *detachment* for basal shear planes, defining the sole of rock-slope failures.

This contribution introduces a classification system based on the pre-avalanche deformation pattern (structural style and geometry) of the rock-slope failure areas. The classification scheme is based on a number of studied cases from crystalline bedrock of Norway, eight of which are described. Each case is evaluated in terms of geometry as well as deformation mode. In the following discussion of presented cases, we focus on issues of importance for stability.

Conceptual model for rock avalanche source areas

Based on pre-avalanche deformation patterns, rock avalanche source areas in Norway can be grouped into: (1) rockfall areas, (2) rockslide areas, and (3) complex fields (Fig. 1). The subdivision is essentially on two criteria: structural geometry and style of deformation. Deformation mechanisms can be ascribed to fall, slide, or complex interactions. Slide commonly occurs in moderate slope gradients (<45°), whereas fall in most cases appears on steep slopes (>60-75°), commonly with a sub-vertical orientation. Complex movements involve slide, block rotation and direct fall.

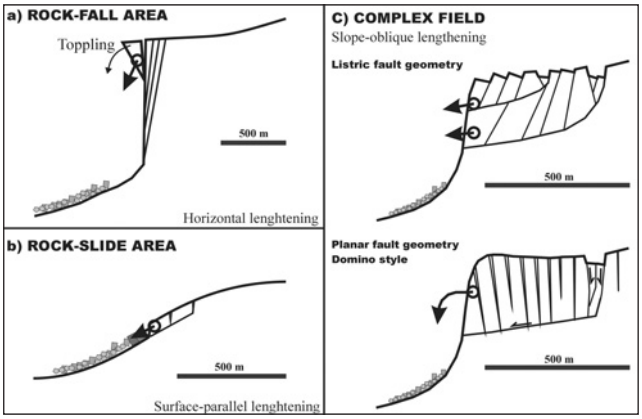

Fig. 1. Geometric model for rock-slope failures, distinguishing between joints, extension fractures, shear fractures and faults (see text for definitions).

Rockfall area

A rockfall area (Fig. 1a) is a type of source area found in steep slope gradients. It is characterised by blocks separated from in situ bedrock by steep, edge-slope-parallel fractures. Fractures with a high angle to the slope commonly limit the block on one or both sides, or split the main block into segments. The lower parts of the fractures may surface in the slope, meaning that the block is kept in place solely by frictional forces along the fracture plane(s). This implies that, when the driving force overcomes the frictional forces, the block immediately accelerates and a free fall is the result. New fractures may form prior to or as blocks are released, leading to a back stepping of the unstable area. Thereby, the source area either consists of one single block or of several blocks separated by sub-parallel fractures. The size of the blocks is variable from some m^3 to several mill. m^3. Large blocks have vertical and horizontal dimensions of the order of several hundred meters. Frequently, the upper part of individual blocks rotate outwards, leading to opening of 1-3 m wide crevasses near the precipice edge. Such rotation is termed *toppling* (Goodman & Bray 1976), and the final failure causes direct fall without sliding.

Rockfall areas constitute a moderate human hazard in that fall-out of single blocks affects limited areas on valley floors. However, large rock-falls potentially develop into full-scale avalanches that may travel for some distance, and in the case of fjords, can create significant tsunamis. The disastrous Tafjord event of 1934 originated from this type of source area.

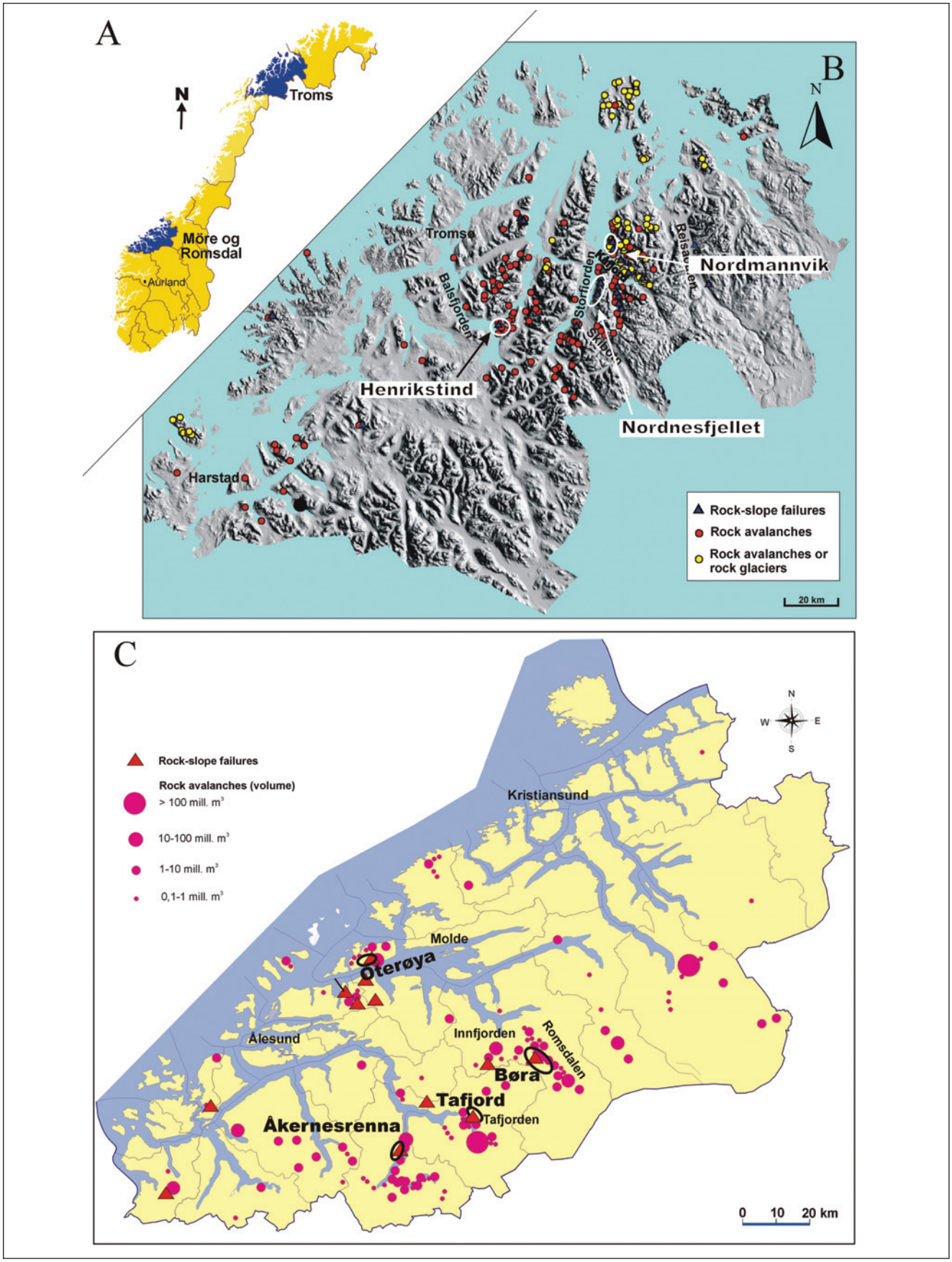

Fig. 2. (A) Outline map of Norway, locating regions with recorded pre-historic rock-avalanches and rock-slope failures. Locations described in the text are situated in the: (B) Troms County of North Norway, Møre & Romsdal and Sogn & Fjordane counties of northern West Norway (C). Modified from Blikra et al. (in press).

Rockslide area

Rockslide areas are found where the slope has a relative low gradient (<45°), and where zones of weakness, for example foliation, layering or pre-existing fractures (e.g., exfoliation), are oriented sub-parallel to the slope (Fig. 1b). Deformation occurs by surface blocks sliding along reactivated, underlying planes. Movements in the lower parts of the slope gradually lead to failures in its upper parts, giving rise to a back and upward stepping process, a mechanism that can develop large in areas covered with angular blocks. Key parameters include block size, slope gradient and the strength of the material on slip surfaces.
Rockslide areas may represent a considerable hazard. Large volumes of loose blocks can be mobilized because of creep over time of large blocks or within block fields. This may lead to instability that at an ultimate stage in the cause of destructive rock avalanches.

Complex field

Complex fields have an extent that commonly exceeds 1 km^2 and a depth varying from 20 to several hundred metres (Fig. 1c). They consist of numerous fault blocks, and partly are characterised by a chaotic and uneven surface morphology. The overall topographic gradient of the source area is relatively low, whereas the bounding mountainside slopes moderately to steeply towards the valley or fjord. Complex fields show an intricate deformation pattern, commonly above one or several detachment levels. They develop lobes separated by distinct transfer faults, where each lobe is deformed independently of those in adjacent areas. In depth, movements along pre-existing planar, low-angle planes (for example foliation, layering, exfoliation, or pre-existing fractures) detach the overlying blocks. Such detachments can be identified by fault gauge and breccia as well as by groundwater seepage along the detachment plane. Internal blocks of the lobes are separated by faults, and are either rotated towards the slope, or into the back-bounding, leading-edge fault. Block-internal segmentation by faults and fractures is common, as are internal graben structures that, in many cases, are found along the innermost part of the collapsing area. The deformation mechanism can be ascribed to a combination of rockslide, rockfall and block rotation (toppling).
Two end-member types of complex fields can be distinguished by variations in style of block movements and fault geometry (Fig. 1c). These are fields with either (i) listric fault geometry or (ii) planar fault geometry. The listric geometry is characterized by downwardly curving master-faults, creating significant internal deformation as blocks rotate and consequently collapse. A common surface configuration is that of horsts and grabens. The planar fault geometry results in a domino-style block configuration. The movements generate cavities and deep clefts, and the blocks remain intact until they reach a critical angle and then collapse internally, or topple. One criterion that separates the two complex fields is the general pattern of block rotation. Listric master faults cause rotation away from the slope and generate block-internal deformation, whereas planar faults lead to intact blocks with minor rotation either towards or away from the slope.
Complex fields involve large volumes of rock that can be triggered to cause a rock avalanche. If the entire field fails synchronously, the effect on the valley floor will be disastrous. The travelling rock-mass will cover large areas, and flow several km down the valley before settling (e.g., Blikra et al. in press). In the case of fjords, flood waves of gigantic dimensions can be expected. Therefore, complex fields constitute a significant hazard to populated areas.

Examples of rock-slope failure

Eight examples of rock-slope failures are presented (Fig. 2). All indicate recent and perhaps on-going movements. The described sites are located in the Troms (North Norway), Møre & Romsdal and Sogn & Fjordane counties (northern West Norway).

Rockfall areas

Two typical rockfall areas involving toppling, at Henrikstind and in Tafjord, are described. They are distinctive, on sub-vertical mountain sides, and with one or more steep crevasse or extension fractures between solid rock and the unstable block along the slope edge.

Henrikstind. - This rockfall area is located at Ørntuv (Fig. 3), east of Balsfjord (Troms County), and is characterised by an unstable, mega-block of approximately 300.000 m^3. Ørntuva is situated 600 m above sea-level (asl), above a sub-vertical (87°), 200 m high cliff-face. Blocky rockfall talus is widespread at the toe of the cliff, where the slope dips moderately to gently towards the sea. Rocks of the area include calcite-mica-schist, garnet-chlorite-schist and various phyllites, conglomerate and marble, all with sub-horizontal foliations. They belong to the Stordals Formation of the Caledonian Lyngen Nappe (Zwaan et al. 1998).
Near the edge of Ørntuva, deep cliff-parallel crevasses are present (Fig. 3), with fracture widths varying between 0.3 and 1.5 m. These are linked to extension fractures trending at a high angle to the cliff-face. All fractures are sub-vertical, and their depth several tens of metres, although this cannot be measured exactly due to infill of colluvium. The traces of fractures, which emerge in the cliff face, indicate the vertical extent of the block (Fig. 3d).

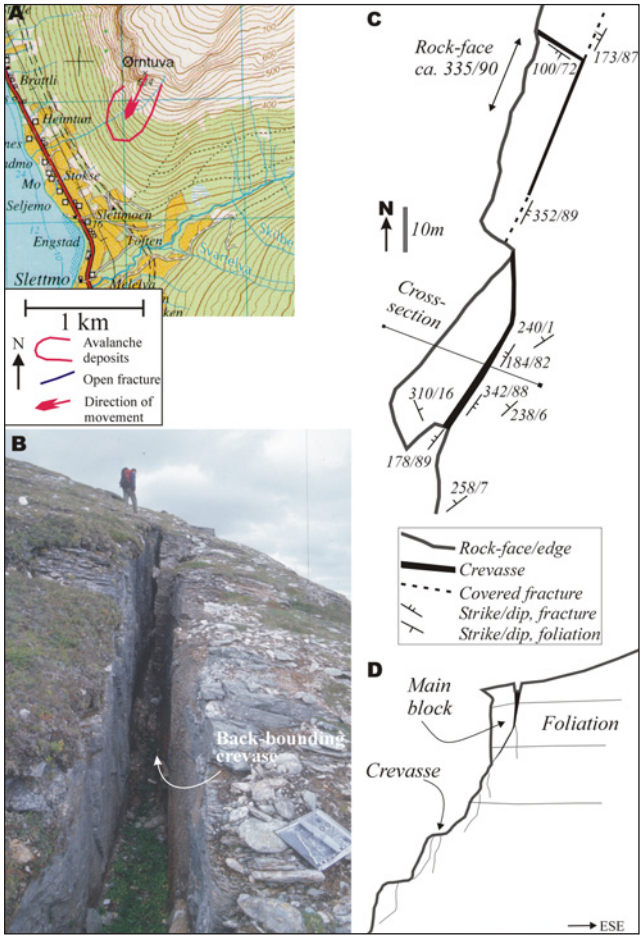

Fig. 3. Henrikstind rockfall area, North Norway. A) Map locating the site for pre-avalanche deformation. B) Photograph of the back-bounding, slope-parallel crevasse that limits the unstable block. View is from the northeast. C) Map outlining the main structures of the site. D) Cross-section of the site (located in C).

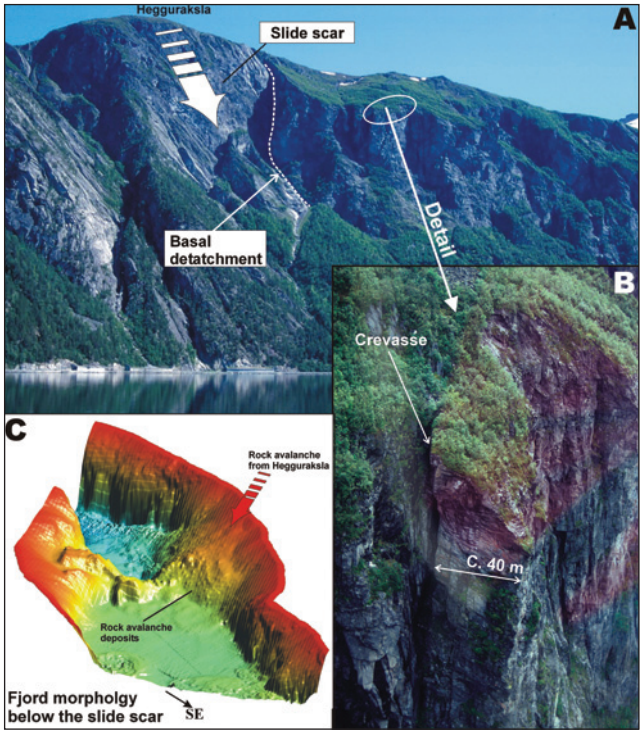

Fig. 4. Tafjord rockfall area, northern West Norway. A) Photograph of the northern mountainside of the Tafjord. Several scars from pre-historic rock-avalanches are seen. A basal detachment, visible in the mountain side, bounds a large plateau that shows signs of deformation. View is from the southwest. B) Photograph of a large block in the cliff face above the Tafjord, located along the outer margin of the mentioned plateau. C) Rock-avalanche deposits at the bottom of the fjord (Blikra et al. in press), which relates to a pre-historic avalanche from the Hegguraksla (photograph in A).

Tafjord. - The Tafjord rockfall area (Møre & Romsdal County) is characterised by a moderate to steep slope below a sub-vertical rock-face from the fjord and up to ca. 800 m asl (Fig. 4). Main rock units are banded mica gneisses, partly quartzo-feltspathic, belonging to the Risberget Nappe (Tveten et al. 1998). In general, the foliation dips steeply to moderately to the south, and slightly oblique to the cliff-face. This structure was important during the rock avalanche of 1934. This is seen by the scar near the base of the avalanche source-area that follows the foliation. Additional slope-parallel and perpendicular, sub-vertical fractures participated in the decoupling and segmentation of the block that avalanched, and is now a boulder fan on the floor of the fjord.

Kaldhol & Kolderup (1936) and Bugge (1937) describe the disastrous avalanche of 1934. Before the avalanche, lower parts of the mountainside were covered by a scree (Heggura scree). Above this, a single large block (Langhammeren block) was separated from stable rocks by fractures and other weakness zones. This block was estimated to be about 150 m high and 200 m wide, with an approximate volume of 3 mill. m^3. This value includes the mobilized scree below. The impact of the avalanche with the sea resulted in a devastating flood wave, which washed more than 60 m above the opposite shorelines, and at the same time the nearby Tafjorden communities were washed away by a c. 15 m high tsunami.

At present, pre-avalanche deformation of Tafjord is revealed by two large blocks and, in addition, by a large plateau behind the blocks that shows some signs of instability (Fig. 4b). The blocks represent a rockfall area in the cliff-face, with individual block volumes of approximately 1-2 mill. m^3. They are bounded by sub-vertical, metre-wide crevasses behind, and restricted and segmented by steep, slope-oblique fractures, consistent geometrically suggesting deformation by a toppling mechanism. At several places, the soles of the blocks can be seen. These consist of steep to moderately inclined, 5-10 cm thick layers of breccia that host smectite-bearing (Grimstvedt et al. 2002) fault gouge.

The inclined plateau behind the blocks shows minor internal fracturing and a vague, back-bounding surface depression in the moraine, suggests fracturing of the underlying rocks. The depression can be followed to a steep, through-going shear plane in the cliff face, containing a 5-15 thick layer of breccia. Farther down, this

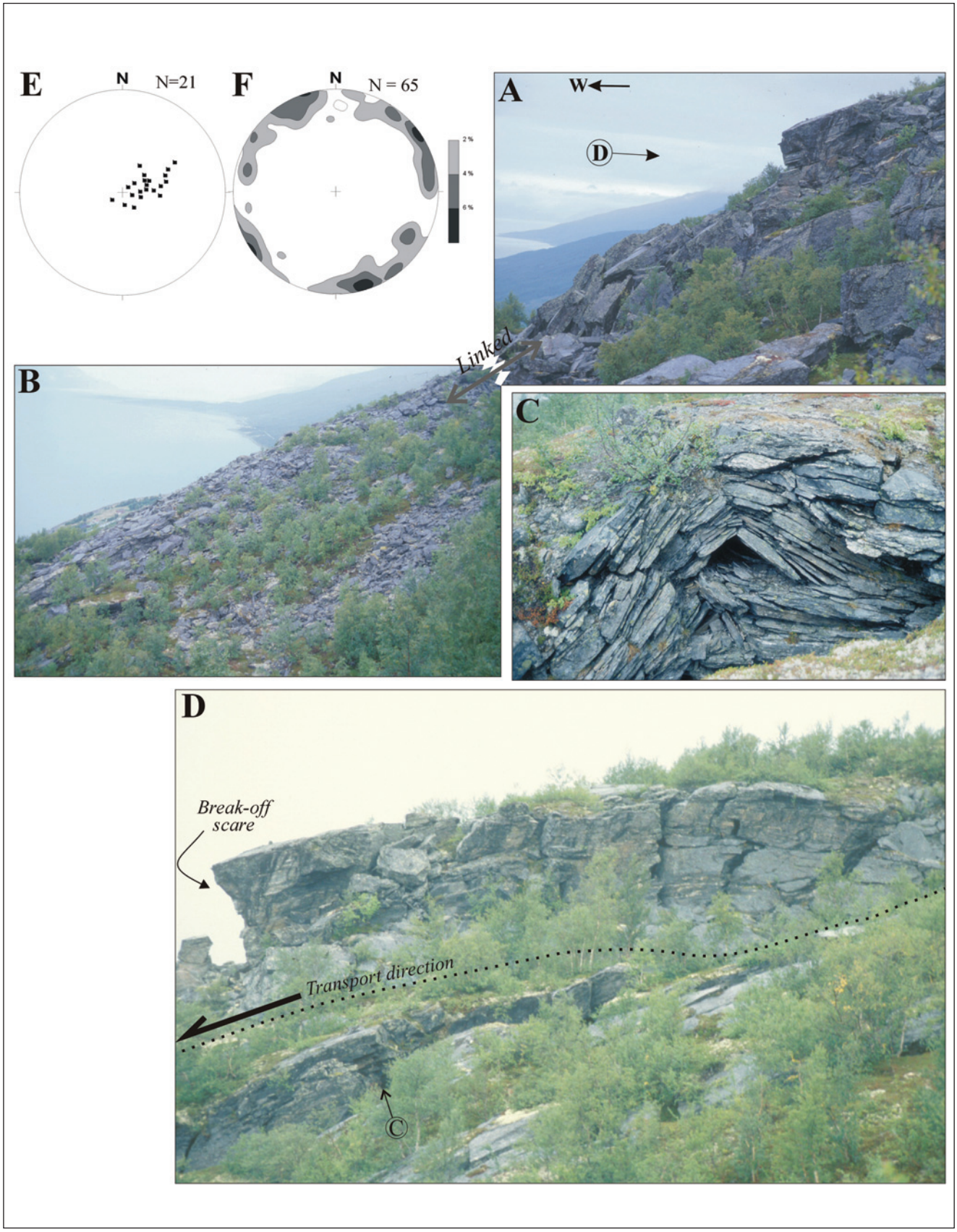

Fig. 5. Nordmannvik rockslide area, North Norway. A)-B) Linked photographs of the upper part of the rockslide area, with highly fractured bedrock in the upper part and large blocks farther down-slope. The lower part of the area is characterized by a field of blocks. C) Kink-fold caused by shear movement along foliation-parallel fractures in the bedrock. D) Close-up photograph of highly fractured bedrock, indicating the location of a shear plane. Note the foliation-controlled steps of vertical fractures in the rock mass. E) Stereoplot of poles to foliation (lower hemisphere, equal area). F) Stereoplot of contoured poles to fractures.

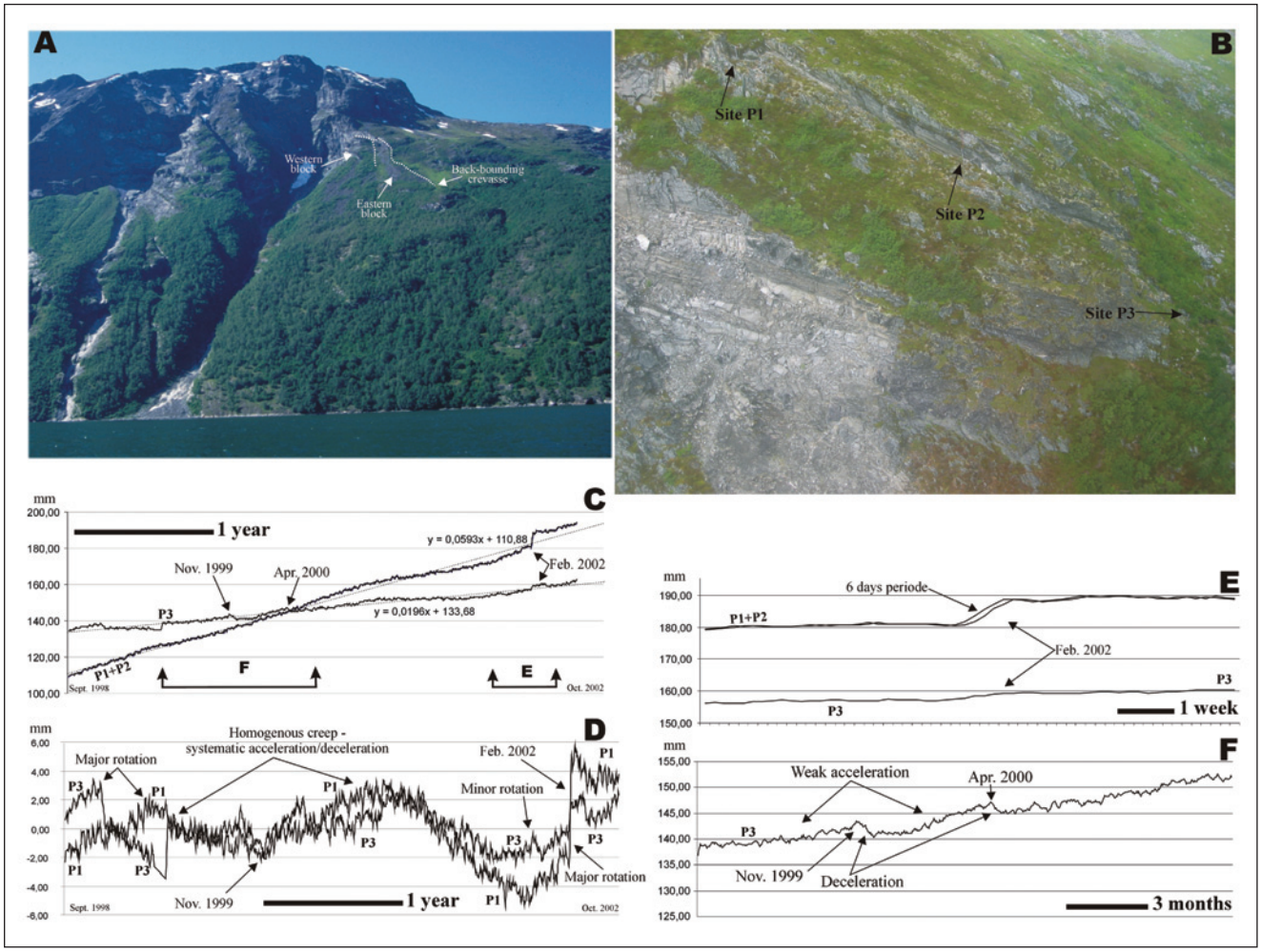

Fig. 6. Åkernesrenna rockslide area, northern West Norway. A) Photograph of the area affected by deformation, as indicated by the arrows. Two blocks have been identified. The mountain slope displays several scars caused by pre-historic rock-avalanches, which seem to have utilized exfoliation surfaces. View is from the north. B) Close-up photograph of the eastern block (see text), which shows the sites monitored in the surveillance program (photograph: Erik Lied, NGI), as discussed in Sandersen et al. (1996). C) Plot that shows cumulative displacement (mm) for three sites (P1, P2 and P3) between September 1998 and October 2002 (data from Stranda Kommune). Noise is reduced through a running average of 5 neighbouring points/recordings. The approximate linear trends for the dataset are indicated. D) Plot of variations in cumulative displacement for P1 and P3, seen as variations around the linear trend line (0-line in the plot), as established above. E) Plot of event in February 2002, showing rapid changes in the movement pattern. F) Plot illustrating long-term and short-term changes recorded at site 3 (P3).

structure merges into the slide scar of an older, major rock avalanche (detachment of Fig. 4a). A rock-volume of approximately 60 mill. m3 can be estimated for this mega-block that can actually classify as an immature complex field.

Rockslide areas

The Nordmannvik and Åkernesrenna sites are typical rockslide areas. They are characterised by a low slope gradient where zones of weakness, oriented sub-parallel to the slope, act as sliding surfaces. They differ in that one area is controlled by the foliation, the other by exfoliation fractures.

Nordmannvik. - This rockslide area is located above the Nordmannvik inlet, on the eastern side of the Lyngen fjord (Troms). It is located at 250-500 m asl on a slope that has an average gradient of 32° (Fig. 5). The bedrock consists of fine grained, partly laminated garnet-quartz-mica-schist and medium-grained amphibolite that occur as metre-thick, foliation-parallel layers. These Silurian rocks belong to the Kåfjord Nappe within the Nordreisa nappe complex (Andresen et al. 1985; Andresen 1988; Zwaan 1988).

The area is characterised by a large field of loose blocks on top of low-angle shear fractures, along which they have been transported. Common block sizes are in the range of some m^3 to more than 100 m3. The basal shear fractures are parallel to the slope and activate the gently to moderately west-dipping foliation (Fig. 5e). The latter has also been reactivated by exfoliation. The importance of the foliation is also documented by foliation-parallel steps of steep fracture walls (Fig. 5d) of joints

and crevasses. Such steep structures separate the blocks. They have a directional preference, with a tendency for slope-parallel or slope-perpendicular orientations (Fig. 5f). These orientations relate to reactivation of pre-existing fracture systems and a weak cleavage in the rock. Many blocks are internally deformed by fracturing or, in one case, shaped into a kink-fold (Fig. 5c). The resulting block field shows several characteristic features. Blocks appear in overlapping lobes, probably reflecting a temporal evolution of the rockslide area. Furthermore, blocks tend to be larger and more intact in the upper parts of the lobes, whereas lower parts show smaller, partly shattered and denser packed blocks.

Åkernesrenna. - This area is located north of Sunnylvsfjord, in Møre & Romsdal County. The deformed slope (Fig. 6a) consists of quartzo-feldspatic gneisses with an overall, steeply south to SE-dipping foliation (Tveten et al. 1998) which is folded around a gently ESE-plunging axis. The basal, controlling structures are likely exfoliation fractures that dip moderately south towards the fjord. This interpretation is supported by the fact that exfoliation surfaces are well developed in the area. The unstable slope is between 525 and 900 m asl, with a total failure area covering approximately 300 000 m^2 (NGI 1989, 1996). It consists of a shattered rock mass with a reported thickness of 15-45 meters, which is transported down a gently (near 35°) sloping mountain side. Annual downhill creep of the order of approximately 4-5 cm has been monitored, and probably started in the 1960's (Sandersen et al. 1996; Larsen 2002). The rockslide area can be divided into western and eastern blocks based on their structural style and partly by their sliding rate. The western block (Fig. 6b), with an estimated rock volume of 1.4 mill. m^3, has been transported approximately 25 m downhill on an average dip angle of 38°. A distinct, 20 m wide and up to 20 m deep graben, caused by movements on extensional fractures, defines the upper boundary of the block. The block is highly fractured, with three sets of steep extensional fractures, and a typical block size between 0.1 and 3 m^3. The fractures have large openings which allow efficient drainage during heavy rainfalls (NGI, 1989).

The eastern block appears in a slope with an average gradient of 33°. Contrary to the western block it is basically un-fractured, and has a volume of c. 4.5 mill. m^3. This block rotates around a axis perpendicular to the slope located in the east, leading to a total down-slope movement exceeding 2 m near the western side of the block (NGI, 1989). The block is limited behind by a joint to the east which gradually opens westwards to be a 2-3 m wide crevasse.

The upward boundary of the deformed area is defined by the mentioned graben with associated extension fractures, and the joint and crevasse, which together separate the two blocks from in situ bedrock. Transport is parallel to the surface, which dips 30-40° to the south (Fig. 6b), and is taken up along one or more slope-parallel exfoliation plane(s) acting as detachment surfaces. Based on numerical simulations, NGI (1996) concluded that the northern block is highly unstable, whereas the western block is stable at low internal water pressures. Also, the northern block can be released in one avalanche, which would result in a tsunami in the fjord below. However, the area is not mapped in detail, and several crucial questions with bearing on the stability assessment remain. These include the interpreted geometry of the field, and the position and gradient of the detachment, both of which affect estimated volumes used in the numerical modelling and tsunami evaluations.

The eastern block is monitored by a continuous, daily surveillance program consisting of three extensometers (sites on Fig. 6b). Details of the monitoring program, and recordings from 1993 to 1995, are discussed in Sandersen et al. (1996). Data from 1998 to 2002 confirm a continuous creep of the block, with slightly higher movement rates at sites 1 and 2 (P1 and P2, Fig. 6c) compared to site 3 (P3). In general, the movement patterns have been linear during the last 4 years, consistent with stable creep. However, local events also appear in the dataset. For example, in February 2002 (Fig. 6e) a 6 day period shows fast acceleration followed by equal deceleration of sites 1 and 2, whereas a minor change is recorded for site 3. This is consistent with internal block deformation, as well as rotation of the entire block around a fixed point on its sole. Also, site 3 shows long periods of weak acceleration followed by short periods of deceleration (Fig. 6f). When the entire dataset is evaluated with respect to variations from the overall linear movement trend, two patterns emerge (Fig. 6d): (i) For a long period the entire block moved homogeneously (c. 750 days). (ii) In two shorter periods, changes in movements have been faster and more complex. This is consistent with periods of either major or minor block rotation. The overall, detailed movement pattern suggests that friction along the sole structure varies both in time and space, and that the block in periods rotates around retardation spots or areas on the basal detachment (see Discussion).

Complex fields

Four complex fields are described; Nordnesfjellet, Børa, Oterøya and Aurland. They show large (km^2) areas of deformation structures a rough topography, and unstable rock volumes exceeding 10 mill. m^3.

Nordnesfjellet. - This complex field is located in the western part of the mountain (Troms County) at around 500-800 m asl (Figs. 7 and 8). The deformed area is 4 km long and 1.2 km wide, with an average slope gradient of 30° above a 300-400 m high, west-facing cliff. Below the cliff, there are lobes of blocky

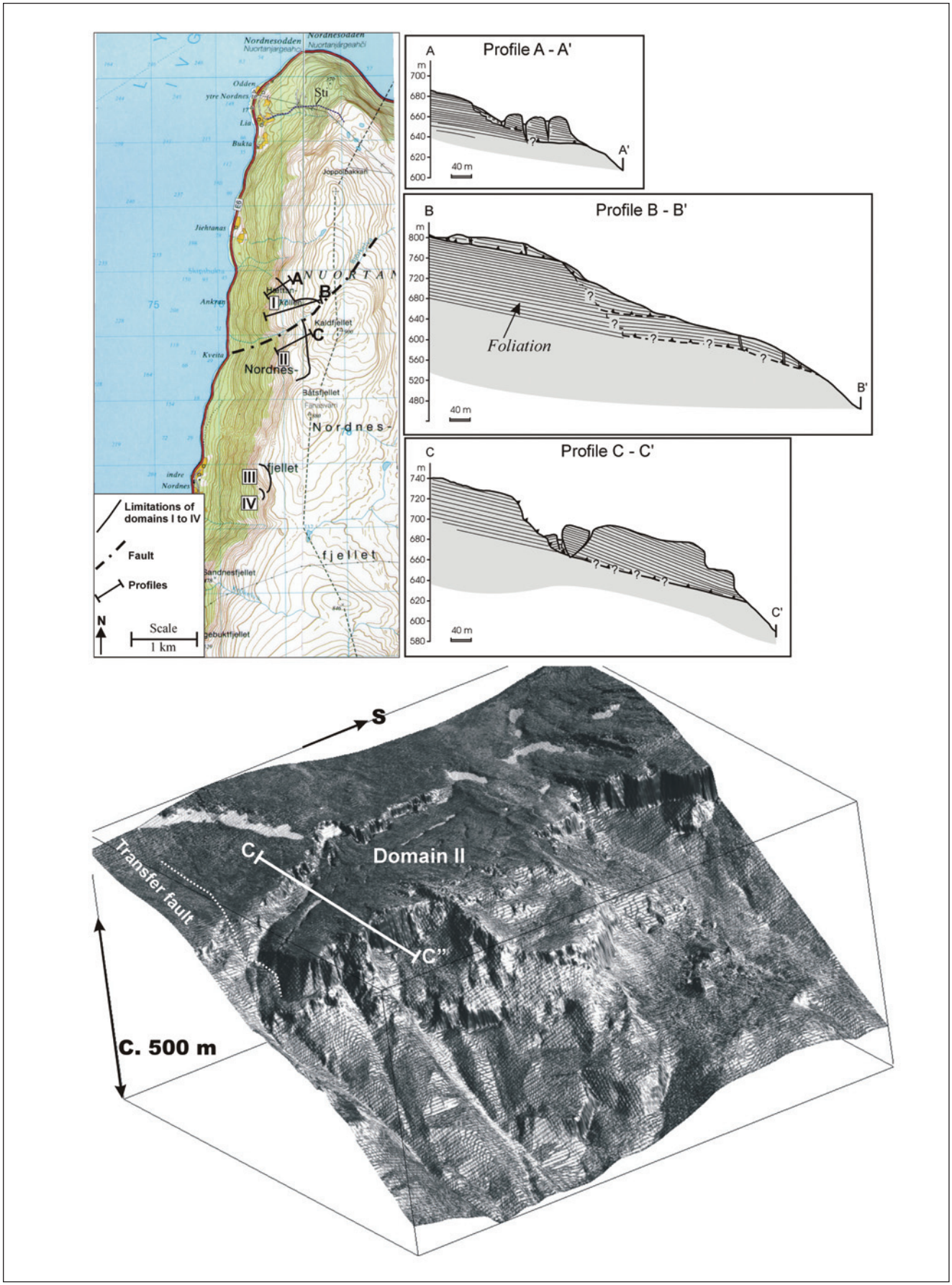

Fig. 7. Nordnesfjellet complex field, North Norway. The map locates the four domains described in the text, and the cross-sections. The 3D-model is based on detailed topographic information, which was used as a baseis for mapping.

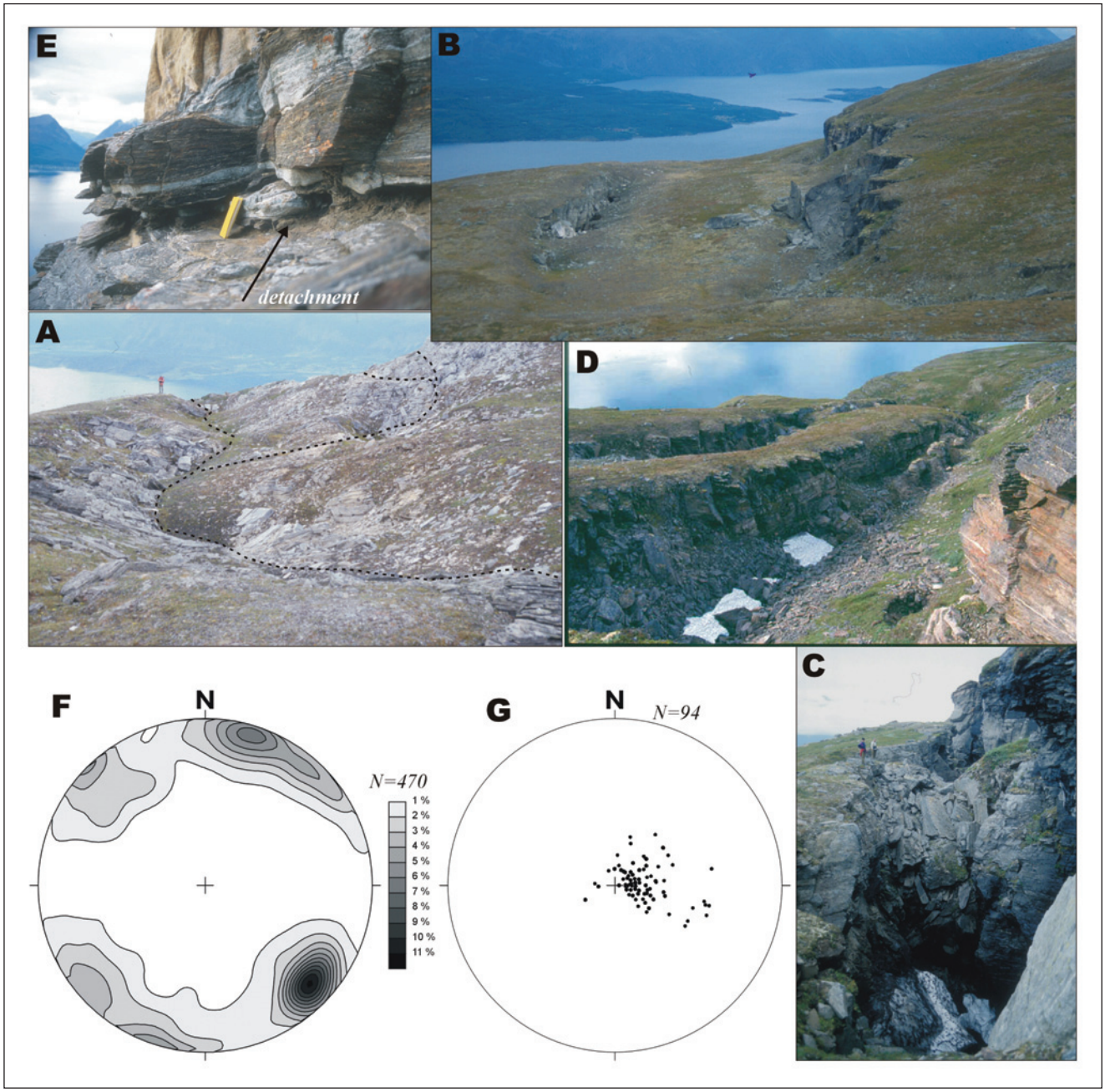

Fig. 8. Nordnesfjellet complex field, North Norway. A) Photograph of surface deformation along the upper boundary of Domain I, seen from the south. B) Photograph of major crevasse and back-bounding fault scarp of Domain II, seen from the southeast. C) Close-up photograph of the domain II fault scarp. D) Photograph of two fault scarps that bound a graben in the northern part of Domain II, viewed from the south. E) Photograph of exposed basal detachment, characterized by breccia and gouge in a 5-10 cm thick layer with groundwater seepage. F) Stereoplot of contoured poles to fractures recorded in the complex field. G) Stereoplot of poles to the foliation in the complex field.

rockfall talus, some reaching the sea. Common rocks of the area are well-foliated amphibolite, dolomite- and calcite marble and garnet-quartz-mica schist of the Kåfjord Nappe (Andresen 1988; Zwaan 1988), which occur in distinct, foliation-parallel layers. The foliation dips gently to the west (Figs. 7, profiles, and 8g), towards the cliff-face, and is slightly steeper near the cliff. The total volume of rock failure is estimated to be between 50 and 100 mill. m^3. An approximately 2 km long, slope-facing fault scarp defines the upper boundary of the complex field (Fig. 8a-d). Other typical structures include large synthetic (towards cliff) and antithetic normal faults, distinct fault scarps, extension fractures and joints, and at least three levels of basal detachment (Fig. 7, profiles). At most places the surface consists of rotated and shattered blocks.

The complex field can be separated into 4 distinct domains, numbered I to IV from the north (Fig. 7a). The two largest domains are located in the north (I and II). They are separated by a pre-existing NE-SW-stri-

king, down to the NW normal fault, which has been reactivated as a transfer structure. The northernmost domain (I) is detached from intact bedrock behind by a normal fault, which runs obliquely to the general topography. Movement on the fault has resulted in the formation of a cleft up to 14 m deep. The hanging wall of the fault is crosscut by extension fractures and smaller listric, normal faults, most of which face the cliff (synthetic), but several also dip eastward (antithetic). Some can be traced as up to 250 m long surface depressions. Closer to the cliff, deformation is more chaotic and intense. In the cliff-face, two low-angle detachments crop out. They consist of fault breccia and gouge, and both leak ground water (Fig. 8e). Three analysed gouge samples all contain smectite and chlorite (Grimstvedt et al. 2002).

Domain II is located south of the above-mentioned transfer fault. A 700 m long fault scarp, running slightly oblique to the cliff-face, bounds the area behind (Fig. 7, profile C-C'). Overall, down to the W separation across this structure is approximately 15 m. In the proximal hanging wall to the scarp there is a 500 m long, 10 m deep, and up to 40 m wide graben (Fig. 8b, c, d) that is bounded by an antithetic fault on the cliff side. Towards the cliff, up to 200 m long, open extension fractures and some listric normal faults are seen. In this cliff-face a basal, low-angle detachment is also exposed.

Two smaller domains, III and IV, are found in the south (Fig. 7a). They resemble the larger structural domains with downhill-facing, concave scarps, which run oblique to the topographic contours. They also show chaotic, blocky areas, albeit deformation here is less pronounced. Domain III displays large, sub-vertical extension fractures, bounding several large blocks in the lower part of the area that have moved by toppling.

The overall geometry is displayed in cross-sections from domains I and II (Fig. 7). In order to explain the general deformation system, including the back-bounding scarps and grabens, block rotation, and hanging wall fracture systems, underlying low-angle detachments are required. These act as deep and/or shallow-seated, mainly foliation-parallel shear surfaces, as observed in the cliff-face parts of the complex field (Fig. 8e).

Generally, the complex field contains two sets of sub-vertical fractures. These strike NE-SW and ESE-WNW (Fig. 8f), and oblique to the N-S striking cliff face. They reactivate pre-existing mineralised fractures that are common in the area. This is further shown by the inherited and reactivated fault that separates domains I and II, which has an orientation similar to the NE-SW-striking fracture set.

Børa, Romsdalen valley. - This complex field (Møre & Romsdal County) constitutes a more than 2-km long plateau located 900 m above the valley floor (Fig. 9). It is bounded by a NE- dipping slope towards Romsdalen that has an average gradient of 37°, increasing to nearly 42° in the upper part. The site is situated in Precambrian, partly migmatitic quartzo-feldspathic gneisses, belonging to the Western Gneiss Region (e.g., Milnes et al. 1997; Tveten et al. 1998). In general, the gneissfoliation strikes E-W and is sub-vertical. However, there are variations in the north due to folding. Large areas of the field are covered by Quaternary till, which has been truncated by faults. In addition, recent GPS monitoring of the field suggests ongoing block movements in its outer part. Because of uncertainties with respect to the depth of the fractures, the total volume is crudely estimated to be between 50 and 200 mill. m^3.

The Børa complex field reveals large, deep crevasses (Fig. 9a, b) that strike almost parallel to the valley slope. These crevasses are in general sub-vertical, but as one approaches the slope, they dip steeply towards the plateau. Fractures are more abundant towards the slope, and some zones of extension fractures and joints are organised in enechelon fashion. At most places, separation of fracture-walls is truly horizontal and nearly wall-normal. A striking graben structure, bounding the field behind, appears c. 200 m from the valley slope. It is defined by two, near-vertical faults with horizontal lengths of 500 m. Locally, the graben is 50 m wide, with a down-throw of the central block varying from 5 to 15 m. Internal faults and shear fractures segment the down-faulted block (Fig. 9c).

The field can be divided into southern and northern sub-areas. In the north, fractures strike mainly WNW-ESE, but there is a spread from E-W to SE-NW. This pattern coincides with the dominant E-W strike of the foliation and pre-existing faults (Fig. 9g, j). The latter are recognised by slickensides coated with epidote and quartz. In the southern sub-area, fractures strike N-S and E-W (Fig. 9f, i). Again, the E-W-striking foliation is important, whereas the N-S strike is controlled by pre-existing fractures and cleavage. The importance of pre-existing fractures can be evaluated based on the background fracturing. Outside the complex field, fractures can be divided into four sets based on orientations (Fig. 9h, k); N-S, E-W, NE-SW, and sub-horizontal. The three first sets are sub-vertical. N-S and E-W fractures coincide with the most prominent fracture orientations in the complex field, suggesting that pre-existing fractures have been reactivated during Quaternary movements. Unexpectedly, the NE-SW fractures, oriented perpendicular to the valley slope, have minimal bearing on the complex field. In conclusion, reactivated foliation (E-W) and foliation-parallel fractures seem to control the structural pattern, whereas fractures oriented perpendicular (N-S) to this, have a subordinate effect.

It is questionable whether or not there is a basal detachment to this complex field, or if the deformation was absorbed by elastic strain at depth. The lengthening of the area is in the range of ca. 5%. Such lengthening should be sufficient to fracture the rock and thereby generate a detachment. Presence of a detachment is also supported by the drainage into fractures of a lake on

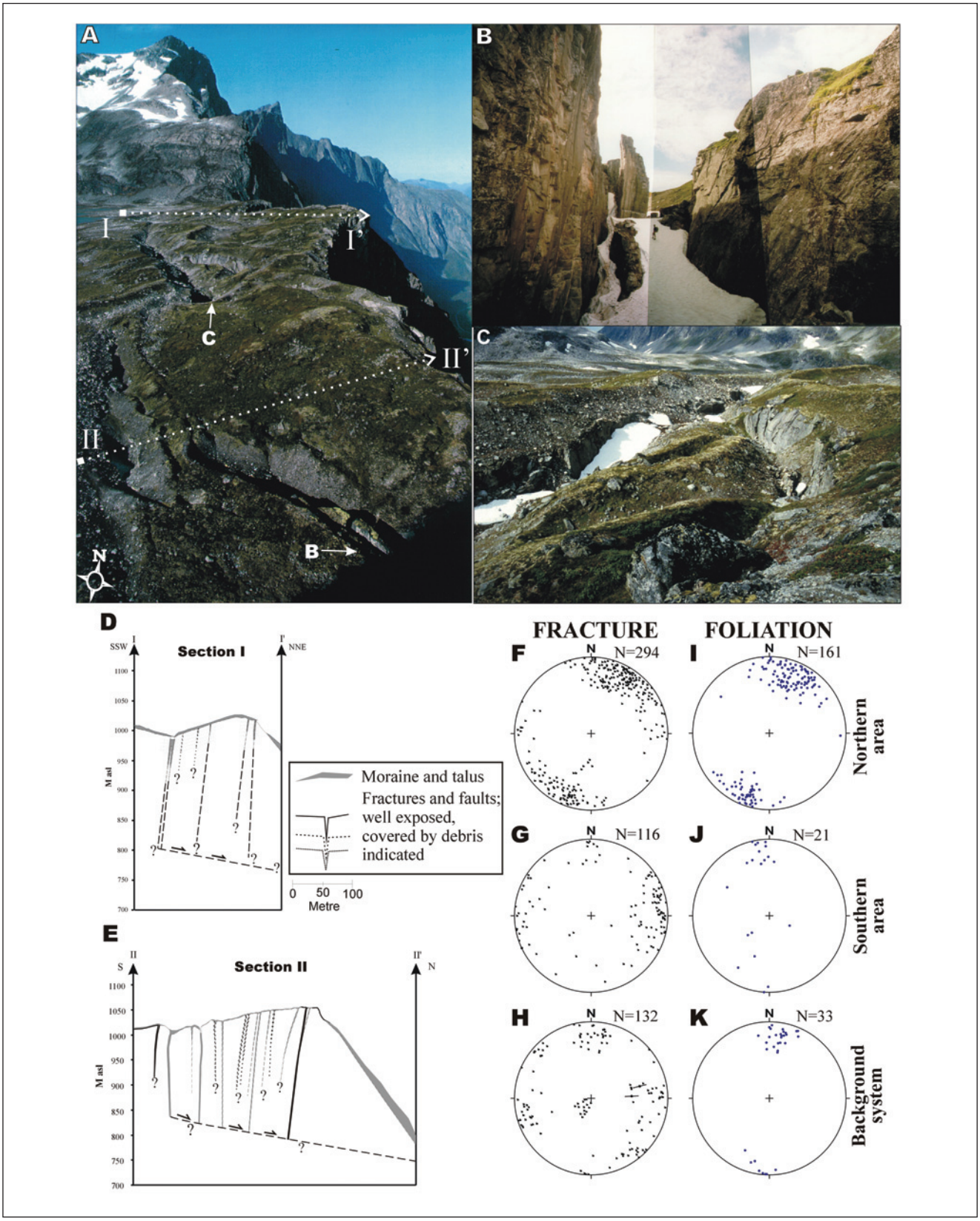

Fig. 9. Børa Complex field, northern West Norway. A) Overview photograph of the Børa complex field, seen from the south. Cross-sections and detailed photographs are located. B) Photo-mosaic of major crevasse. Note person for scale. View is from the south. C) Photograph of graben found along the back-bounding scarp. View is from the south. D) Cross-section I-I', with inferred basal detachment at depth. E) Cross-section II-II', with inferred basal detachment at depth. F) Stereo-plot of poles to fractures recorded in the northern part of the complex field. G) Stereo-plot of poles to fractures recorded in the southern part of the complex field. H) Stereoplot of poles to fractures recorded outside the area affected by the complex field. I) Stereoplot of poles to foliation recorded in the northern part of the complex field. J) Stereoplot of poles to foliation recorded in the southern part of the complex field. K) Stereoplot of poles to foliation recorded outside the area affected by the complex field.

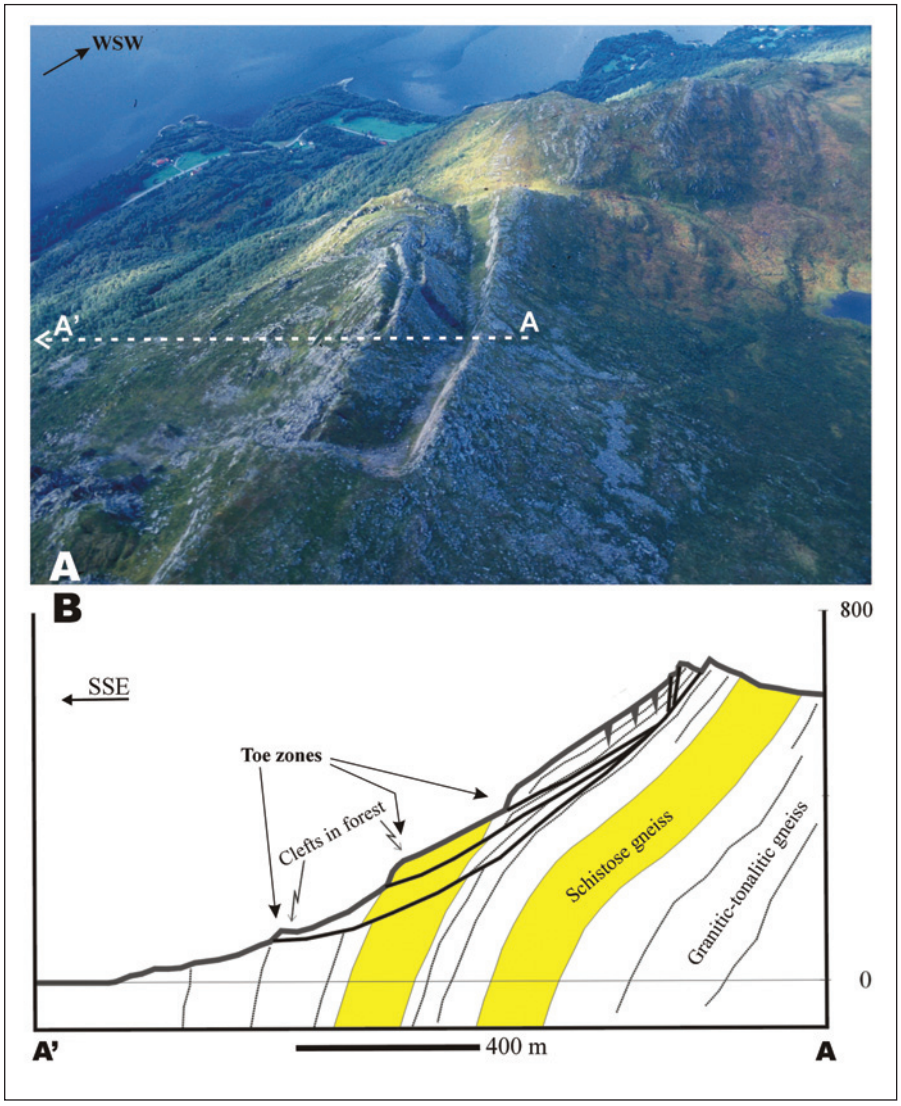

Fig. 10. Oterøya complex field, northern West Norway. A) Photograph of the complex field, looking SW. B) Cross-section of the complex field, showing various basal shear surface levels interpreted from surface observations. The toe-zones probably represent detachments emerging at the surface, or alternatively, reduced displacement along the detachment (propagation folds) or steps (ramps) in the detachment at deeper levels.

top of the complex field, and which likely emerges as groundwater springs lower down in the valley slope. Based on this reasoning, as well as the structural style, the area is classified as a planar styled complex field.

Oterøya. - The Oterøya complex field (Møre & Romsdal County) is seen in an approximately 1 km wide and up to 700 m high slope (Fig. 10), stretching from a near-shore level up to the peak of Oppstadhornet. The estimated volume of the field is in the range of 10 mill. m^3 (Blikra et al. 2001; Bhasin & Kaynia 2004). It is characterised by crevasses and clefts reflecting block movements in various quartzo-feldspatic gneisses, some mica-rich and schistose (Robinson et al. 1997; Blikra et al. 2001). The field is bounded by three main structures; an upward bounding master fault and two marginal faults to the southwest and northeast. The master fault is clearly displayed as an escarpment, up to 20 m high, forming a half-graben (Fig. 10). This fault is superimposed on the steeply SE-dipping foliation as well as a narrow zone of cataclasite and carbonate-cemented fault breccia (Blikra et al. 2001). The south-western marginal fault strikes NW-SE and dips steeply NE. It is seen as a fracture zone, which reactivates an older fault. This structure is a transfer fault marked by down-oblique sliding. In the east, the termination of the complex field is seen as a NNW-SSE striking and steeply SW dipping fracture zone, which acted (or acts) as a transfer structure.

Internally, the complex field is segmented into large blocks by two sets of steep fractures (mainly faults), which strike NW-SE and NE-SW. The NE-SW set is sub-parallel to the master fault and the foliation in the rocks. The fault sets are different in that they show slope-oblique (down to the S) transport on the NW-SE fractures and down-slope (down to the SE) transport on the NE-SW fractures. The slope-oblique transport could relate to lateral ramps in the underlying detachment. Many of the blocks in the field are rotated. Some surface blocks rotate out from the slope, in addition to the general down-hill sliding, whereas the overall pattern of the complex field is that of rotation towards the slope above one or more detachment. The geometry and position of the detachments are indicated by topo-

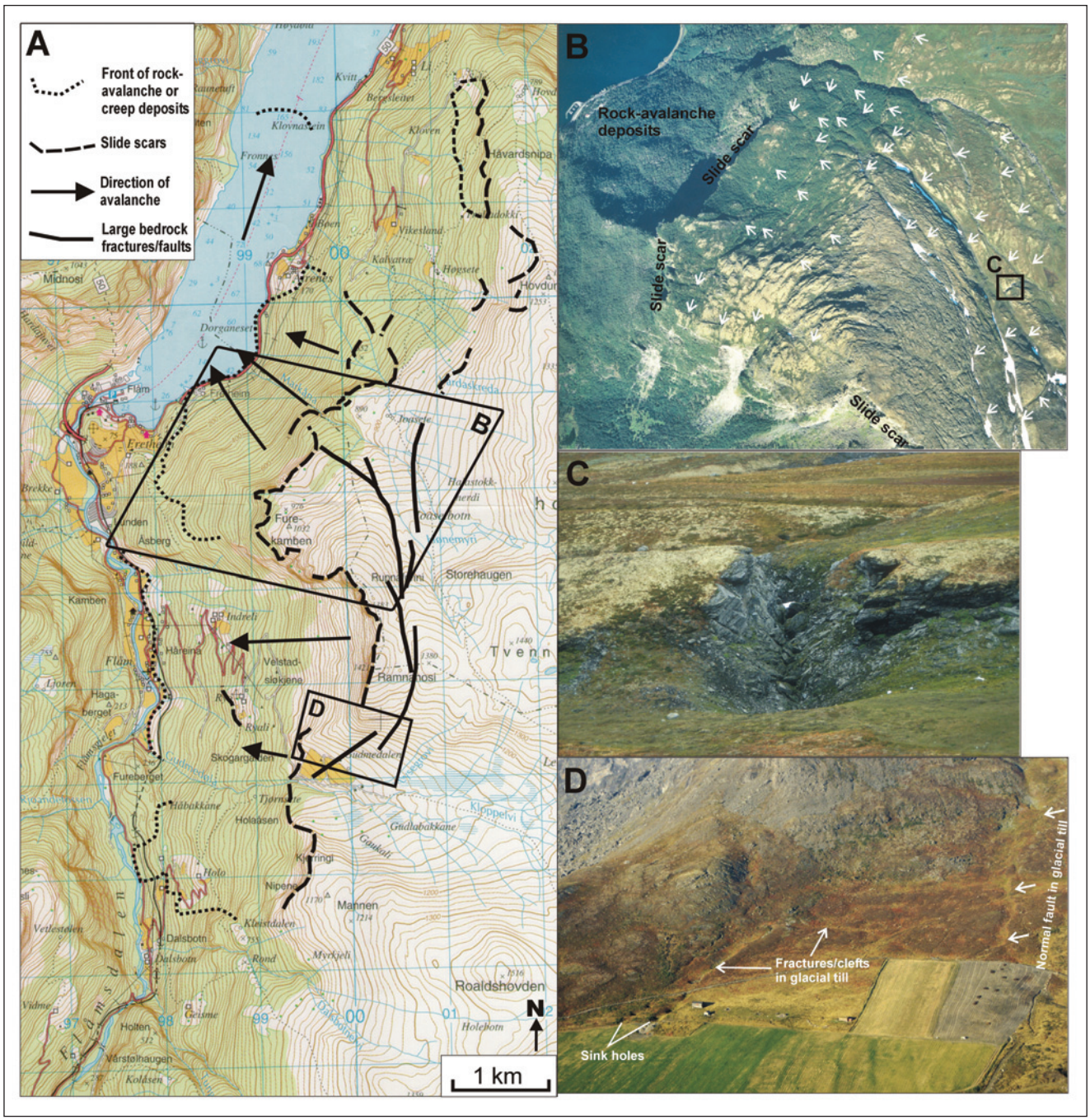

Fig. 11. Aurland Complex field, West Norway. A) Map showing main features of the complex field (locating B and D). B) Aerial photograph showing major faults (arrows), slide scars, and pre-historic rock avalanche(s). C) Photograph of cross-crevasse that links two faults, seen from the southwest (located in B). D) Photograph of faults and sinkholes, viewed from the south.

graphic irregularities, or "toe-zones". In the profile these zones are interpreted as locations where the detachments cut up to the surface (Fig. 10b).

In the lower part of the mountain slope, two deep clefts appear approximately 10 m above low cliffs. They define grabens with down-faulted blocks that have sunk 2 to 5 m. The importance of this is that it suggests deep-seated movements of the entire slope down to sea level, and that a basal detachment for the overlying complex field probably surfaces in this area (Fig. 10b).

Northeast of the mega-block, near Oppstadhornet, there are indications of other instabilities. In the steep slope, there are moderately sized blocks (c. 100.000 m^3) bounded by shear fractures that reactivate the steeply SSE dipping foliation. These blocks have slid 10-30 m down-slope without significant internal fragmentation. There are also hundreds of metres long, 1-2 metre-wide, slope-parallel depressions and crevasses in the moraine on top of the mountain ridge.

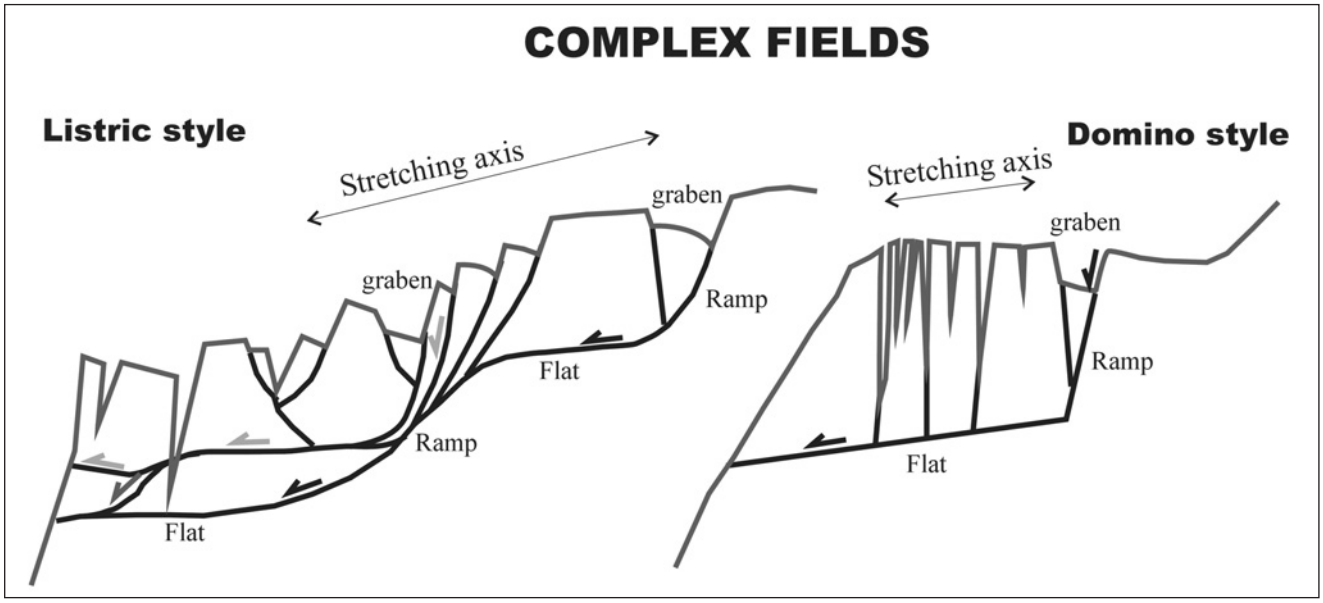

Fig. 12. Geometric models for complex fields, addressing the difference in cross-sectional geometry of fault systems of listric style and domino style fields. Note that hanging wall extension fractures and joints are mainly located above detachment flats, whereas faults occur above ramps of the underlying detachment.

Aurland. - In the soft, dark phyllites of the Aurland-Flåm region (Sogn & Fjordane County), there are a number of instability features within an 11 km long zone. This area also contains widespread bouldery rock-avalanche deposits (Fig. 11; e.g., Blikra et al. 2002). The area is located on the eastern valley side, where the foliation dips moderately west, towards the valley. Monitoring of movements near the valley floor shows periodical creep that is closely linked to precipitation (Domaas et al. 2002).

Pre-avalanche deformation is seen as a series of normal faults and associated half-grabens, locally with an en-echelon pattern. On the plateau, some faults are marked by sinkholes (Fig. 11d). In the south, the back-bounding structure is a 4 km long normal fault, seen as a distinct 1-2 m high scarp. Farther north, this fault separates into segments that are slope-parallel and W-dipping. These shows down-slope shear movements by reactivation of the foliation. In the north, several N to NNW striking faults and joints, parallel to the steep mountainside, interact with a series of E-W, transverse fractures (Fig. 11c). Near the valley floor, there are 100-700 m wide boulder-dominated lobes, which are most likely formed by creep of rock-avalanche deposits (Blikra et al. 2002). Similar features also occur along and in the Aurlandsfjord.

The structural pattern shows that the entire mountainside west of the back-bounding composite fault has moved several metres down towards the west in the direction of the valley (Blikra et al. 2002). Basal detachments have not been observed in the area due to thick overburden in the form of rock-avalanche deposits and moraine. However, assuming that a deep-seated detachment follows the foliation of the phyllites from the valley to the back-bounding fault scarp, the gradient of this structure will be less than 22°. This means that a total volume of 900-1500 mill. m^3 is unstable.

Discussion

Comparison of structural styles

The presented classification diagram, describing typical rock-slope failures (Fig. 1), constitutes a tool for characterizing pre-avalanche deformation. One has to keep in mind that there are transitional types as well as variations within the same type. Reviewing the bedrock lithologies of the described sites, varying from diverse quartzo-feldspatic gneisses, to mechanically weaker schists, phyllites, meta-conglomerates and marbles, it is clear that lithology alone does not control rock-slope failures. However, soft schist at some sites (e.g., Aurland) seems to be characterised by a distinct style of deformation, with lower shear angles and creep in lobes. This geometry and behaviour have clear similarities to numerous schist-dominated sites elsewhere in the world (e.g., Crosta & Agliardi 2003). A general pattern is that the internal structural fabric (foliation, cleavage) of the rocks in our study clearly affects the structural geometry. In addition, reactivation of fractures plays a role. The slope gradient is also an important factor (e.g., Nicoletti & Sorriso-Valvo 1991).

The complex fields reveal structures consistent with low-angle, overall slope-oblique lengthening, basically controlled by the orientation of the basal detachment (Fig. 12). At Nordnesfjellet, which is an end-member

example, the structural geometries are consistent with listric style master faults. This is seen as both syn- and antithetic normal faults with distinct fault scarps, extension fractures and joints, several basal detachments, and large areas showing rotated fault blocks (Figs. 7 and 8). From a geometric point of view, joints and extension fractures seem to dominate above smooth, low-angle detachment planes (flats), whereas shear fractures and normal faults dominate above ramps of the detachments. Such ramps can be identified by steps in the topography. Also, ramps cause collapse of the overlying blocks. Analysis of the structural geometry of the Nordnesfjellet complex field suggests that the scarps link to one or more underlying low-angle detachments, which act as deep-seated, mainly foliation-parallel shear surfaces. This is evidenced by fault gouge with smectite and breccia along exposed low-angle, foliation-parallel detachments (Fig. 8e), and also by ground water seepage.
In the Børa complex field, faults are planar (Fig. 9). The most prominent structure is a graben behind, bounded by steep faults and, in addition as one approaches the slope, open extension fractures. A downward bounding detachment is inferred at depth. By comparing the Nordnesfjellet and Børa complex fields, it is clear that overall lengthening basically is parallel to the detachment, which is the controlling structure. Hence, the stretching axis is slightly oblique to the surface topography and highly oblique to the mountainside (Fig. 12).

When the various pre-avalanche deformation sites are compared, distinct differences are evident. The Henrikstind and Tafjord rockfall areas are situated above cliff faces, and are bounded by sub-vertical crevasses and extension fractures consistent with horizontal lengthening. The Nordmannvik and Åkernesrenna rockslide areas are situated in mountain slopes with a moderate gradient. Block movement occurs on surface-parallel detachments along foliation or exfoliation surfaces that are oriented sub-parallel to the slope, and blocks are bounded by steep to vertical extension fractures and joints. The pattern is that of slope-parallel lengthening. This is in contrast to the complex fields, where the stretching axis has a gentle plunge and is subparallel to the underlying detachment. It follows that the overall difference in lengthening direction reflects the differences in slope gradient combined with the reactivated, pre-existing structural grain. Thus, moderate slope gradients (25-50°) generally lead to lengthening parallel to the slope, whereas steep slope gradients (>50°) trigger near-horizontal lengthening. Pre-existing planar structures are important and especially the foliation of the rocks (e.g., Hermanns & Strecker 1999) which forms potential planes of reactivation.

Complex fields involve rock volumes that exceed 10 mill. m^3, and cover areas larger than 1 km^2 in extent. They seem to be rare, though complex fields are not unique to Norway. Similar structures are described from Scotland (Ballentyne 2002) and Canada (Bovis 1990). An example from Canada includes a 300 mill. m^3 rock massif that is involved in slow, gravity-driven movement. Similar to our observations, Bovis (1990) observes extension fractures, grabens and scarps, and a basal, deep-seated shear zone is inferred as the controlling sole structure. Likewise, Bovis & Evans (1995, 1996) and Agliardi et al. (2001) describe large collapsing fields with extension fractures, grabens, linear trenches and scarps. Angeli et al. (2000; see also Chigira & Kiho 1994) have monitored large blocks in the Giau Pass, Italy. Characteristically, a large graben is localised to the upper part of the slope, and megascopic blocks move on a sub-horizontal slip surface.

Deformation mechanisms and driving forces

Rock avalanches are initiated when the shear stress overcomes the shear strength of the rock mass. Terzaghi (1962) argued that the critical angle for rock slides in slopes underlain by massive rocks with a random joint pattern is about 70°. Carson & Kirby (1972) infer the critical slope angle to be 45° to 75°. Such slope angles are higher than those observed for several of the described sites (30-42°), indicating that several mechanisms and forces assist during deformation. This is certainly the case for the complex fields, which develop above gently to moderately inclined detachments. Shorter-term forces relate to: (1) seismic activity, (2) water pressure and lubrication, (3) glacial debutressing, and (4) frost-related processes. We thereby exclude human activity, erosion and biological factors (e.g. root wedging) from the discussion.

Seismic activity. - Earthquakes have triggered numerous rock avalanches in historical times (e.g. Solonenko 1977; Adams 1981; Whitehouse & Griffiths 1983; Keefer 1984; Maharaj 1994; Schuster et al. 1996; Wieczorek & Jager 1996; Hermanns & Strecker 1999). For Norway, there are only a few examples of avalanches triggered by earthquakes, although rockfalls and minor clay slides were observed during the earthquake in Rana in 1819 (M 5,8-6,2; Muir Wood 1989). This mechanism has also been suggested for the offshore Storegga slide (Bryn et al. 2002). The neotectonic Berill Fault (Anda et al. 2002) in Møre & Romsdal County shows development of a complex field in the hanging wall, suggesting that there is a link between rock-slope failures and earthquakes. Similarly, concentrations of both pre-historical rock avalanches and rock-slope failures to certain zones (Blikra et al. 2001, 2002) suggest a semi-regional triggering mechanism, such as an earthquake, albeit indirect dating of avalanches in the fjords may point to repetition rather than to a single major event (Blikra et al. in press).
Earthquakes larger than magnitude (M) 5.5 are rare in Norway, and occur along certain major structures (e.g.,

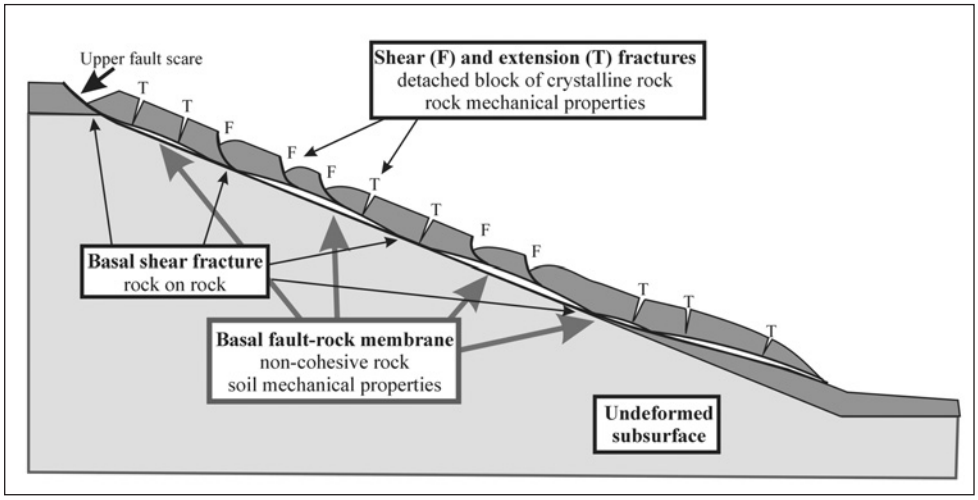

Fig. 13. Profile illustrating a two-layer model for pre-avalanche deformation in a rock-slope failure area. Text-boxes describe factors and mechanical properties that have to be evaluated in stability assessments.

Dehls et al. 2000a,b; Fejerskov et al. 2000; Lindholm et al. 2000). Earthquakes of M6.0 are regarded as a minimum for triggering rock avalanches (Keefer 1984; Jibson 1996). Such magnitudes have not been instrumentally recorded in Norway, but could have caused avalanches in pre-historic times. Anda et al. (2002) discuss the importance of major earthquakes for triggering synchronous avalanche events, reasoning that the spatial distribution of rock avalanches can be used to constrain pre-historic earthquakes. With the present knowledge regarding both the cause for - as well as the timing of rock-slope failures, we are not able to distinguish between the influence of major palaeoseismic events and other factors.

Water pressure and lubrication. - Water is regarded as an essential component in gravitative mass movement processes, either as an important agent to mineral breakdown or growth, or as a contributor to lubrication, or even as an active force (Terzaghi 1950). In general, a rise in pore pressure reduces the effective normal stress, thereby reducing the shear resistance of the slide surface. Further, water increases the weight, thereby adding to the driving force. A water column will also exert outward pressure on a rock mass, encouraging block overturning (Carson & Kirby 1972). In any case, fatigue due to variations in water pressure (Carson & Kirby 1972) lowers the safety factor of rock-slope failures (e.g., Keller 1992). In Norway, water pressure increases during snow melting and heavy seasonal rain periods (e.g., Sandersen et al. 1996), especially within well-developed fracture networks. For several sites in Norway characterized by down-slope creep of rocks, build-up of water pressure is regarded as fundamental for movements (Bjerrum & Jørstad, 1968), as discussed for the Aurland schists (Domaas et al. 2002), and indicated for the Åkernesrenna site (Sandersen et al. 1996).
Lakes on the Børa complex field have no outlets, hence large volumes of rain and melt water drain through the open fracture network of the plateau, and probably re-emerge in springs close to the valley floor. This suggests that the intra-rock water column is 2-400 m high, if not immediately drained, which is less likely in a partly soil-clogged fracture aquifer. Consequently, the groundwater column probably acts as a significant force on the fracture system. In a general context, building up a significant groundwater pressure requires the water to be partly or fully trapped. The most likely way to seal a rock-slope failure area from underlying, fractured bedrock is by the formation of a low-permeable membrane along the basal detachment. Two types of membrane are likely - an ice sole, common in permafrost regions, or a fault-rock sole. The latter is brought about by shear movements, crushing wall-rock minerals/grains (asperites) and rock pieces into very fine-grained, non-cohesive fault rocks (gouge and breccia; e.g., Sammis et al. 1987; Blenkinsop 1991; Braathen et al., in press), which may or may not be chemically altered. A through-going or semi-continuous fault-rock membrane not only trapps fluids, it constitutes a weak layer with significantly lower shear strength than the surrounding rocks. Therefore, it is probably a prerequisite for deformation by stable creep (e.g., Petley & Allison 1997). In a strength context, non-cohesive gouge and breccia have mechanical properties more like those of soft sediments (soil), and should be treated as such in stability assessments (Fig. 13).

Glacial debuttressing. - Glacial processes influence the rock stability such that glacial erosion steepens rock slopes. Another effect related to glaciations is the removal of the support provided by adjacent glacier ice during periods of down wastage, i.e. glacial debuttressing. The consequent stress-release is thought to be of major importance for rock-slope stability in glaciated regions (see McSaveney 1993; and review by Ballantyne 2002). This is because loading under the weight of the overlying ice will induce internal high stress levels both on the valley floor and within the valley slopes. Release of elastic strain energy during periods of ice down-wasting results in propagation of the internal fracture networks, which may cause rock-slope failures. Few stu-

died rock-avalanche deposits in Norway were deposited on glaciers (Blikra, unpublished data), suggesting that few immediate rock-slope failures took place during the gradual deglaciation. However, a much better time control of individual events is required in order to conduct a thorough evaluation. Also of importance is that this process can be considerably delayed due to time-dependent dissipation of residual stresses within the rock mass (Wyrwoll 1977; Ballantyne 2002). The relatively young ages of the rock-slope failures in the inner fjord areas of Møre & Romsdal County (Blikra et al., in press) indicate other effects than glacial deloading. On the contrary, some dated rock avalanches in North Norway and in the coastal region of Møre & Romsdal indicate that these events followed shortly after the deglaciation (Blikra et al. in press). Stress-release due to removal of the support provided by glacier ice during the deglaciation phase may thus have been an important factor for rock-slope failures in certain areas.

Frost-related processes. - Frost wedging, in other words the expansion due to freezing of water, creates a significant force. Frost wedging can cause further opening of fractures. Hence, ice wedging can be an important factor causing rockfalls and rockslides. In complex fields, the complexity and low-angle structural pattern require more than frost wedging and gravity as driving forces.
In a broader context, the presence of frozen ground is a vital factor in the stability of mountain slopes since, in most cases, thawing of ice-filled fractures leads to a rapid loss of shear strength. Several studies have shown that frost shattering is most effective at temperatures well below 0°C, preferably below -3 to -5°C (e.g., Walder & Hallet 1985). Matsuoka (1990) especially argues for the importance of water migration during freezing. For Norwegian cases, Sandersen et al. (1996) point out that periods affected by freeze-thaw processes seem to coincide with periods of faster pre-avalanche deformation. In any case, there is a general consensus that frost wedging in rock slopes characterized by freezing assisted by supply and migration of water, is important for stability. Parts of the mountainous regions of Norway are still influenced by permafrost (Etzelmüller et al. 1998; Isaksen et al. 2002). Since melting of permafrost affects the stability of rock slopes (e.g. Haeberli 1992), both past and future melting of permafrost have to be considered when analysing pre-avalanche deformation and failure mechanisms.

Deformation mechanisms and detachment strength

Creep is a relatively slow process that in many cases occurs prior to rock-avalanching (e.g., Petley 2002; Crosta & Agliardi 2003). This is well illustrated by a disastrous avalanche in Vaiont, Italy (Semenza & Ghirotti 2000; Erismann & Abele 2001), which caused flooding of a hydro-electric dam and of a populated valley. At Åkernesrenna, monitored pre-avalanche deformation relates to creep with a fairly stable overall rate (Fig. 6c-f), as is also recorded for a number of sites worldwide (e.g., Petley et al. 2002; Crosta & Agliardi 2003). On the other hand, a detailed analysis reveals both long-term velocity fluctuations and short-term rotational events. Since the sliding block is entirely detached from in situ, surrounding rock by steeply inclined fractures and a detachment, rotation has to be caused by changing shear resistance along the basal detachment. This could relate to several factors such as availability of water (rainfall, snow melting), freeze-thaw processes (Sandersen et al. 1996), as well as features along the detachment itself. The rotation axis appears to both migrate and jump through time, suggesting that resistance to sliding changes along the detachment. Possible causes for this are: (i) inhomogeneous drainage of water of the block and sole, (ii) various mechanical properties of non-cohesive fault rock material(s) along the sole, or (iii) retardarory areas on the sole, for example where rock rests on rock along a surface otherwise covered by a fault rock membrane. Such areas could migrate due to the mobility of soft, water-saturated fault gouge, allowing the overlying block to ground at various places over time (Fig. 13).
In order to trigger creep in an unstable area, the total forces acting on the basal sliding surface have to overcome the critical friction. Two common mechanisms for reduced friction, acting either isolated or in harmony, are; (I) increased pore fluid/water pressure along the shear surface, and (II) weathering and/or abrasion of rocks and clasts/fragments along the shear surface. These processes are time dependent; hence stability evaluations for a given time are temporally unreliable. Increased water pressure reduces the normal stress on the shear surface, thereby reducing the shear resistance. Creep in this context means that sliding starts at a critical value of pore pressure, and that this pressure is maintained in a stable stress situation. More likely, the creep process involves a sudden drop in pore pressure below the critical value when movement takes place and some fluids are drained off, at least locally. Hence, captured pore pressure is released during microscopic slip events, which appear repeatedly in a stick-slip process (Brace & Byerlee 1966; Sibson 1977). If the pressure is increased, rather than maintained or released, the slip event will develop and may even accelerate (Crosta & Agliardi 2003) and, in some cases, such as for Vajont (Italy), evolve into a full-scale rock avalanche (Petley 2002). Alternatively, some mechanism may hinder the development, for example an obstacle at the toe of or underneath the sliding rock body (retard point). Another mechanism is strain hardening along the basal shear surface, for example by changes in fault rock properties (e.g., Braathen et al., in press). For many sites there appears to be a stable velocity of creep that is

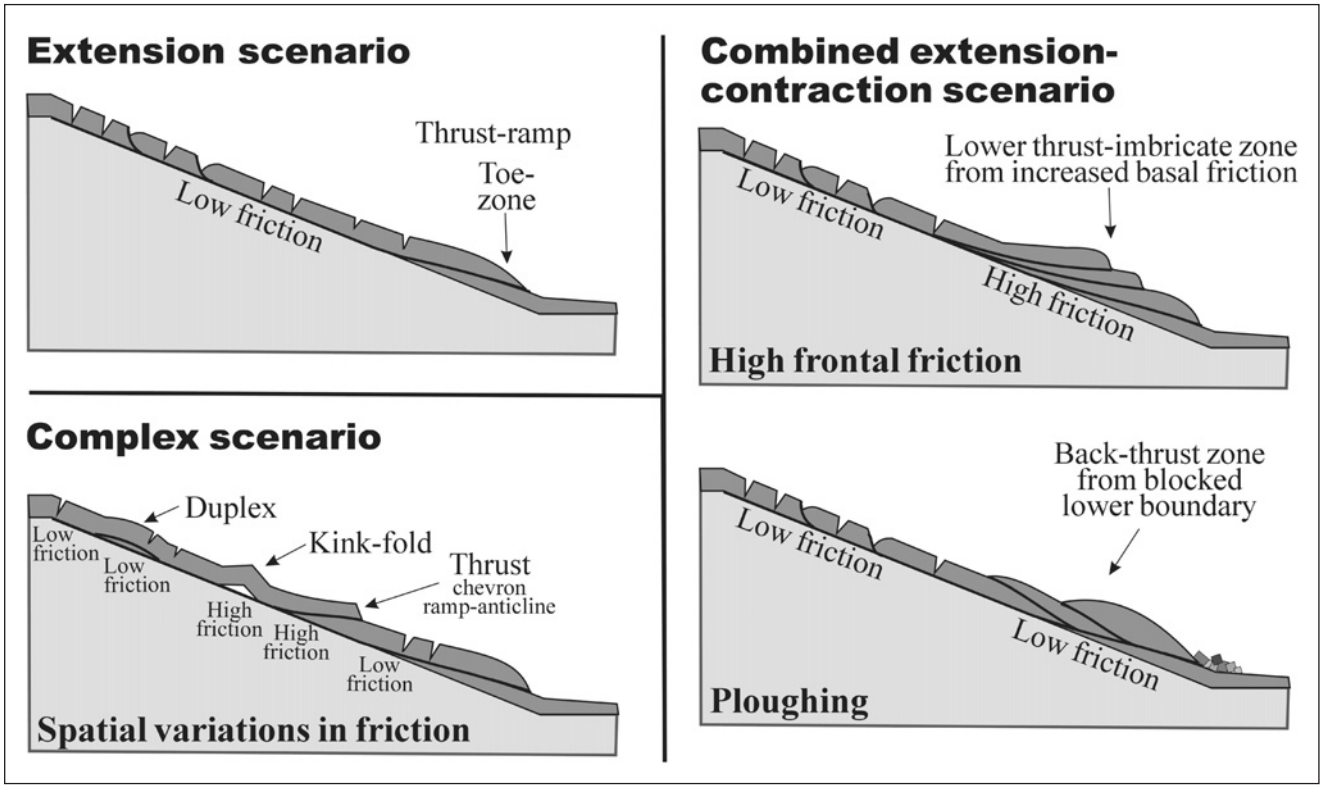

Fig. 14. Schematic profiles illustrating pre-avalanche deformation structures in a rock-slope failure area. Joints, extension fractures and faults are shown. The latter can be subdivided into normal faults and reverse/thrust faults, which are diagnostic for extensional and contractional settings, respectively. Variables include basal friction and blocking of the lower boundary of the field. See Eberhardt (2002) for discussion of numerical models related to intra-block stresses and fracture formation.

reached after acceleration (e.g., Petley 2002; Crosta & Agliardi 2003). This is suggested by the data from Åkernesrenna (Fig. 6c-f), and discussed for Oterøya (Blikra et al. 2001; Harbitz 2002) and implies stable sliding where all forces are in balance.

Weathering and abrasion of or along the basal shear plane can take place in two ways (e.g., Bruhn et al. 1994): (a) Mechanical and/or chemical breakdown of small obstacles (asperites and grains/clasts), which are stress localizers on the surface, thereby enhancing its smoothness, commonly resulting in reduced friction. (b) Chemical alteration of fractured and damaged minerals or grains on or near the shear surface. This may result in the formation of clay minerals. Mechanically weak clays will reduce the shear resistance, as suggested for the detachments of the Nordnesfjellet and Tafjord sites, where smectite has formed in the fault gouge. In any event, slip results in the destruction of minerals and clasts on the basal shear surface (Blenkinsop 1991), which progressively develops into a soft layer of crushed rock (gouge and breccia). A critical strength boundary will develop when the fault rock becomes matrix-supported instead of clast-supported, a development related to progressive strain (Braathen et al. in press). For rock-slope failures, this boundary will be approached as movement increases on sliding surfaces. In addition, progressive development of a breccia or gouge layer, especially if it becomes continuous, has the potential to reduce dramatically the stability of a collapsing mountainside.

One can envisage that the disastrous rock avalanche of Tafjorden in 1934 was caused by gradual changes in strength along the basal sole structure. As described above, narrow zones of breccia appear along scars of pre-historic rock avalanches in the mountainside (Fig. 4). Most of these breccias contain smectite with noticeably low shear strength. In this perspective, gradual alteration of gouge and breccia into clay probably reduced the shear strength of the sole material, thereby playing an important role for the developing rock-slope failure and the subsequent rock avalanche.

Diagnostic structures

Pre-avalanche deformation structures observed within rockslide areas and complex fields can provide insight into intra-block stress conditions, which are controlled by boundary conditions such as friction along the basal shear surface (Fig. 13). With a basis in numerical modelling, Eberhardt (2002) proposed three stress-fracture pattern scenarios. In Figure 14, we further explore these scenarios, relating distinctive structures of the deforming area or field to stress conditions:

1. *Extension scenario* - the entire field under tension

(low basal friction), with diagnostic structures including joints, extensional fractures and normal faults. A lower 'toe-zone' develops when the basal detachment breaks towards the surface, giving rise a near slope-parallel thrust geometry.

2. *Combined extension-contraction scenario* - upper part of the field under tension (low basal friction), revealed by joints, extension fractures and normal faults; lower part under compression seen as stacking of blocks by thrusting, which can be applied to one of the following scenarios: (i) High friction along the basal surface, related to synthetic thrust imbrications, or (ii) ploughing, explained by compression in lower parts due to blocking of the toe, with distinctive (antithetic) back-thrusts.
3. *Complex scenario* - variable parts of the field under compression and tension from spatially changing basal friction, with diagnostic features including contractional structures such as reverse faults and/or kink-folds, as well as extensional features including joints, shear fractures and normal faults.

Structures diagnostic for the various scenarios are well exemplified by the described pre-avalanche deformation sites. Most sites show stretching structures consistent with the Extension scenario (e.g., Åkernesrenna, Nordnesfjellet, Børa). For example, at Oterøya the complex field reveals upper stretching structures and lower 'toe-zones' (Fig. 10), consistent either with the Extension scenario thrusts-ramps (Fig. 14) or with thrust-imbrications within a combined Extension-Contraction scenario. A similar setting is suggested for the Aurland complex field (Fig. 11), where lobes in schist towards the base of the field suggest contractional deformation near the lower boundary, probably related to Ploughing. Another example is the kink-fold observed in the Nordmannvik slide area (Fig. 5c), which is consistent with buckling due to localised contraction in a Complex scenario.

Timing of pre-avalanche deformation

In order to address the hazard related to rock-slope failures, it is critical to establish the timing of deformation and especially to confirm if it is ongoing or not, since ongoing deformation is consistent with evolving instability (e.g., Crosta & Agliardi 2003). Involvement of glacial tills at all described pre-avalanche deformation sites clearly documents post-glacial activity. More importantly, recorded creep, where such data exist (Børa, Åkernesrenna), and local rupturing of the vegetation cover, which is observed at most described sites, suggests that deformation is ongoing. This contradicts arguments for permafrost and glacial processes as important mechanisms or causes of avalanching, although knowledge about permafrost distribution is still rather scarce in Norway. Similarly, melting of glaciers in valleys, leaving steep mountainsides unsupported (McSeveney 1993; Ballantyne 2002), is consistent with peak avalanche activity immediately following deglaciation. This may be the case for some sites of North Norway (Troms County), but is not constrained by ages for pre-historic rock-avalanches of western Norway (Blikra et al. in press), where avalanche activity spans the last 11.000 years.

At the moment, a number of pre-avalanche deformation sites, many in inhabited areas, still remain questionable with respect to timing of deformation. Therefore, in order to establish reliable hazard assessments of deforming mountain sides, two aspects seem crucial: establishment and calibration of more sophisticated stability models, and extensive monitoring programs.

Conclusions

(i) Extensive studies of Norwegian rock-slope failure areas support a subdivision into three principle types: (1) Rockfall areas, (2) rockslide areas, and (3) complex fields. The classification is based on structural geometry and style of deformation, slope gradient, and volumes involved.

(ii) Pre-avalanche deformation is caused by gravity, assisted by short-termed factors such as seismic activity, water pressure and/or frost-related processes, and long-term factores such as gradual changes in the shear resistance of the sole structure. Water pressure and/or frost wedging presumably cause rockfalls, while gradually changing strength in combination with water pressure and freeze-thaw processes in the basal detachment are probably critical aspects in rockslide areas and complex fields.

(iii) Characteristic geological features of rock-slope failures suggest a subdivision into two layers: one is the detached block with intra-block deformation seen as both shear and extension fractures and joints, the other the basal shear fracture (rock on rock) or non-cohesive fault rock layer (membrane) above non-deformed bedrock. This two-layer framework is required in more sophisticated stability modeling, which necessitates evaluation of both rock-mechanic (fracture) and soil-mechanic (fault rock) properties.

Acknowledgements: - The Geological Survey of Norway, Norsk Hydro ASA, the National Fund for Natural Damage Assistance, and the Møre & Romsdal, Troms, and Sogn & Fjordane counties have sponsored the work summarized herein. We especially thank Stranda Kommune/District, which supported us with data from monitoring of the Åkernesrenna site. We are also grateful to Einar Anda, and NGU colleagues (John Dehls, Oddvar Longva) and NGI colleagues (Rajinder K. Bhasin, Ulrik Domaas, Carl Harbitz, Elin Skurtveit) for fruitful discussions concerning geohazards. We appreciate the reviews by E. Eberhardt and J.O. Larsen, which were useful for improvements of the manuscript.

References

Adams, J. 1981: Earthquake-dammed lakes in New Zealand. *Geology 9,* 215-219.

Agliardi, F., Crosta, G. & Zanchi, A. 2001: Structural constraints on deep-seated slope deformation kinematics. *Engineering Geology 59,* 83-102.

Anda, E., Blikra, L.H., & Braathen, A. 2002: The Berill fault - first evidence of neotectonic faulting in southern Norway. *Norwegian Journal of Geology (NGT) 82,* 175-182.

Andresen, A. 1988: Caledonian terranes of Northern Norway and their characteristics. Trabajos de Geologia 17, 103-117.

Andresen, A., Fareth, E., Bergh, S.G., Kristensen, S.E. & Krogh, E. 1995: Review of Caledonian lithotectonic units in Troms, north Norway. *In* Gee, D.G. & Sturt, B.A. (eds.), *The Caledonian Orogeny - Scandinavia and related areas,* 569-578. John Wiley & Sons Ltd.

Angeli, M.-G., Pasuto, A. & Silvano, S. 2000: A critical review of landslide monitoring experiences. *Engineering Geology 55,* 133-147.

Ballantyne, C.K. 2002: Paraglacial geomorphology. *Quaternary Science Reviews 21,* 1935-2017.

Bhasin, R. & Kaynia, A.M. 2004. Static and dynamic simulation of a 700-m high rock slope failure in western Norway. *Engineering Geology 71,* 213-226.

Bjerrum, L. & Jørstad, 1968: Stability of rock slopes in Norway. N*orwegian Geotechnical Institute Publication 79,* 1-11.

Blenkinsop, T.G. 1991: Cataclasis and processes of particle size reduction. *Geophysics 136,* 59-86.

Blikra, L.H., Anda, E. & Longva, O. 1999: Fjellskredprosjektet i Møre og Romsdal: Status og planer. *Norges geologiske undersøkelse Report 99.120,* 21 pp.

Blikra, L.H., Anda, E., Braathen, A., Stalsberg, K. & Longva, O. 2002: Rock avalanches, gravitational bedrock fractures and neotectonic faults onshore western Norway: Examples, regional distribution and triggering mechanisms. *Norges geologiske undersøkelse Report 2002.016,* 48 pp.

Blikra, L.H., Braathen, A., & Skurtveit, E. 2001: Hazard evaluation of rock avalanches; the Baraldsneset-Oterøya area. *Norges geologiske undersøkelse Report 2001.108,* 33 p.

Blikra, L.H., Longva, O., Braathen, A. & Anda, E., Dehls, J. & Stalsberg, K. in press: Rock-slope failures in Norwegian fjord areas: examples, spatial distribution and temporal pattern. In Evans, S.G., Scarawcia Mugnozza, G., Strom, A.L. & Hwemanns, R.L. (eds.), Massive rock slope failure: new models for hazard assessment. Kluwer, Dodrecht. Bovis, M. J. 1990. Rock-slope deformation at Afflication Creek, southern Coast Mountains, British Columbia. *Canadian Journal of Earth Sciences 27,* 243-254.

Bovis, M. J. & Evans, S. G. 1995. Rock slope movements along the Mount Currie "fault scarp", southern Coast Mountains, British Columbia. *Canadian Journal of Earth Sciences 32,* 2015-2020.

Bovis, M. J. & Evans, S. G. 1996. Extensive deformations of rock slopes in southern Coast Mountains, southwest British Columbia, Canada. *Engineering Geology 44,* 163-182.

Braathen, A., Osmundsen, P.T. & Gabrielsen, R.H., in press: Dynamic development of fault rocks in a crustal-scale detachment; an example from western Norway. *Tectonics.*

Brace, W.F., & Byerlee, J.D. 1966: Stick-slip as a mechanism for earthquakes. *Science 153,* 990-992.

Bruhn, R.L., Parry, W.T., Yonkee, W.A., & Thompson, T., 1994. Fracturing and hydrothermal alteration in normal fault zones. *Pure and applied geophysics 142,* 609-644.

Bryn, P., Berg, K. & Lien, R. 2002: Submarine slides on the Mid-Norwegian Continental Margin – a challenge to the oil industry. *Abstracts and proceedings of the Norwegian Geological Society 2-2002,* 25-31.

Bugge, A. 1937: Fjellskred fra topografisk og geologisk synspunkt. *Norsk Geografisk Tidsskrift VI,* 342-360.

Carson, M. A. & Kirby, M. J. 1972: *Hillslope form and process.* Cambridge University Press, Cambridge.

Chigira, M. 1992: Long-term gravitational deformation of rocks by mass rock creep. *Engineering Geology 32,* 157-184.

Chigira, M. & Kiho, K. 1994: Deep-seated rockslide-avalanches precedes by mass rock creep of sedimentary rocks in the Akaishi Mountains, central Japan. *Engineering Geology 38,* 221-230.

Costa, G.B. & Agliardi, F. 2003: Failure forecast for large rock-slides by surface displacement measurements. *Canadian Geotechnical Journal 40,* 176-191.

Domaas, U., Rosenvold, B.S., Blikra, L.H., Johansen, H., Grimstad, E., Sørlie, J.E., Gunleiksrud, O., Engen, A. & Lægreid, O. 2002: Studie av fjellskred og dalsidestabilitet i fyllittområder (Report to the Norwegian Research Council). *Norwegian Geotechnical Institute Report 20001132-32.*

Dehls, J., Olesen, O., Bungum, H., Hicks, E.C., Lindholm, C.D. & Riis, F. 2000a: Neotectonic map: Norway and adjacent areas. *Norges geologiske undersøkelse.*

Dehls, J.F., Olesen, O., Olsen, L. & Blikra, L.H. 2000b: Neotectonic faulting in northern Norway; the Stuoragurra and Nordmannvikdalen faults. *Quaternary Science Reviews 19,* 1447-1460.

Eberhardt, E. 2002: From cause to effect - using numerical modelling to understand rock slope instability mechanisms. *In* Evans, S.G. & Martino, S. (eds.), *Massive rock slope failure: new models for hazard assessment,* 27-31. NATO advanced research workshop, Italy, June 2002.

Eisbacher, G.H. 1979: Cliff collapse and rock avalanches (sturzstroms). *Canadian Geotechnical Journal 16,* 309-334.

Erismann, T.H. & Abele, G. 2001: *Dynamics of Rockslides and Rockfalls.* Springer-Verlag Berlin Heidelberg New York.

Etzelmüller, B., Berthling, I. & Sollid, J.L. 1998: The distribution of permafrost in southern Norway – a GIS approach: *In* Proceedings of the 7th International Conference on Permafrost, Yellowknife, Canada, 23-27 June. *Nordicana 57,* 251-258.

Fejerskov, M., Lindholm, C., Larsen, B.T. & Nøttvedt, A. 2000: Stress map, North Atlantic area, scale 1:3 million. Integrated basin studies, Dynamics of the Norwegian Continental margin. *Geological Society of London Special Publication 167.*

Goodman, R. E. & Bray, J. W. 1976: Toppling of rock slopes. *ASCE Speciality Conference in Rock Engineering of Foundations and Slopes 2,* 201-234. American Society of Civil Engineering, Boulder, Colorado.

Grimstvedt, A., Karlsen, A.E. & Braathen, A. 2002: XRD analyses of rock-failure sole-rocks. *NGU analysis report 2002.0444,* 8 pp. + appendices.

Haeberli, W. 1992: Construction, environmental problems and natural hazards in periglacial mountain belts. *Permafrost and Periglacial Processes 3,* 111-124.

Harbitz, C. 2002: Ormen Lange - Ilandføringsalternativer. Rock slide generated tsunamis - Run-up heights at Barlaldsnes and Nyhamn. *Norwegian Geotechnical Institute Report 20001472-2.*

Hermanns, R. L. & Strecker, M. R. 1999: Structural and lithological controls on large Quaternary rock avalanches (sturzstroms) in arid northwestern Argentina. *Geological Society of America Bulletin 111,* 934-948.

Hungr, O., Evans, S.G., Bovis, M.J. & Hutchinson, J.N. 2001: A review of the classification of landslides of the flow type. *Environmental & Engineering Geoscience VII,* 221-238.

Hutchinson, J. N. 1968: Mass movement. *In* Fairbidge, R. W. (ed.), *Encyclopedia of Geomorphology,* 688-695. Reinhold, New York.

Hutchinson, J. N. 1988: General report: Morphological and geotechnical parameters of landslides in relation to geology and hydrogeology. *In* Bonnard, C. (ed.), Proceedings, *5th International Symposium of Landslides 1,* 3-35. Balkema, Lausanne, Switzerland.

Isaksen, K., Hauck, C., Gudevang, E., Ødegård, R.S. & Sollid, J.L. 2002: Mountain permafrost distribution in Dovrefjell and Jotunmeimen,

southern Norway, based on BTS and DC resistivity topography data. *Norwegian Journal of Geography 56,* 122-136.

Jibson, R.W. 1994: Using landslides for Palaeoseismic analysis. *In* McCalpin (ed.), *Paleoseismology.* International geophysics series 62, 397-438. Academic press.

Keefer, D. K. 1984: Landslides caused by earthquakes. *Geological Society of America Bulletin 95,* 406-421.

Keller, E. A. 1992: *Environmental Geology.* Macmillan Publishing Company, New York.

Larsen, J.O. 2002: *Some aspects of physical weather related slope processes.* Dr. Ing. Thesis, Norges teknisk-naturvitenskaplig universitet, 68 pp.

Lindholm, C.D., Bungum, H., Hicks, E. & Villagran, A. 2000: Crustal stress and tectonics in Norwegian regions determined from earthquake focal mechanisms. *Geological Society of London Special Publication 167,* 429-440.

Maharaj, R. J. 1994: The morphology, geometry and kinematics of Judgement Cliff rock avalanche, Blue Mountains, Jamaica, West Indies. *Quarterly Journal of Engineering Geology 27,* 243-256.

Matsuoka, N. 1990: Mechanisms of rock breakdown by frost action: an experimental approach. *Cold Regions Science and Technology 17,* 253-270.

McSaveney, M.J. (1993) Rock avalanches of 2 May and 6 September 1992, Mount Fletcher, New Zealand. *Landslide News 7,* 2-4.

Milnes, A.G., Wennberg, O.P., Skår, Ø. & Koestler, A.G. 1997: Contraction, extension and timing in the South Norwegian Caledonides: The Sognefjord transect. *In* Burg, J-P. & Ford, M (eds.), Orogeny through time, *Geological Society of London Special Publication 121,* 123-148.

Muir Wood, R. 1989: The Scandinavian Earthquakes of 22 December 1759 and 21 August 1919. *Disasters 12,* 223-236.

Nemcok, A. 1972: Gravitational slope deformation in high mountains. 24th International Congress, Montreal, 132-141.

Nicoletti, P.G. & Sorriso-Valvo, M. 1991: Geomorphic controls of the shape and mobility of rock avalanches. *Geological Society of America Bulletin 103,* 1365-1373.

NGI. 1989: Stabilitetsvurdering omkring Remnane ved Åkernes i Stranda. *Norwegian Geotechnical Institute,* Report 85494-2, 20 pp.

NGI. 1996: Åkernes landslide. Numerical simulation of the Åkernes landslide using the universal distinct element code. *Norwegian Geotechnical Institute,* Oslo, 18 pp.

Petley, D.N. 2002: Patterns of acceleration for large slope failures. *In* Evans, S.G. & Martino, S. (eds.), *Massive rock slope failure: new models for hazard assessment,* 110-113. NATO advanced research workshop, Italy, June 2002.

Petley, D.N. & Allison, R.J. 1997: The mechanics of deep-seated landslides. *Earth Surface Processes and Landforms 22,* 747-758.

Petley, D.N., Bulmer, M.H. & Murphy, W. 2002: Patterns of movement in rotational and translational landslides. *Geology 30,* 719-722.

Radbruch-Hall, D. H. 1978: Gravitational creep of rock masses on slopes. *In* Voight, B. (ed.), *Rockslides and avalanches 1: Natural phenomena,* 607-657. Elsevier, Amsterdam.

Robinson, P., Tveten, E. & Blikra, L.H. 1997: A post-glacial bedrock failure at Oppstadhornet, Oterøya, Møre og Romsdal: a potential major rock avalanche. *NGU Bulletin 433,* 46-47.

Sammis, C., King, G. &Biegel, R. 1987: The kinematics of gouge deformation. *Pageophysics 125,* 777-812.

Sandersen, F., Bakkehøi, S., Hestnes, E. & Lied, K. 1996: The influence of meteorological factors on the initiation of debris flows, rockfalls, rockslides and rockmass stability. *In* Senneset (ed.), *Landslides,* 97-114. Balkema, Rotterdam.

Schuster, R. L., Nieto, A. S., O´Rourke, T. D., Crespo, E. & Plaza-Nieto, G. 1996: Mass wasting triggered by the 5 March 1987 Ecuador earthquakes. *Engineering Geology 42,* 1-23.

Semenza, E. & Ghirotti, M. 2000: History of the 1963 Vaiont slide: the importance of geological factors. Bulletin of Engineering Geological Environments 59, 87-97.

Sibson, R.H. 1977: Fault rocks and fault mechanism. *Journal of the Geological Society, London 133,* 191-213.

Solonenko, V. P. 1977: Lamdslides and collapses in seismic zones and their prediction. *Bulletin of the International Association of Enginge-ering Geology 15,* 4-8.

Ter-Stepanian, G. 1963: On the long-term stability of slopes. *Norges Geotekniske Institutt 52,* 1-14.

Terzaghi, K. 1950. Mechanisms of landslides. Application of Geology to Engineering Practice, Berken volume, 83-123. *Geological Society of America Bulletin.*

Terzaghi, K. 1962: Stability of steep slopes on hard unweathered rock. *Geotechnique 12,* 251-270.

Tveten , E., Lutro, O., Thorsnes, T. 1998: Bedrock map Ålesund, M 1:250 000. Geological Survey of Norway.

Varnes, D. J., Radbruch-Hall, D. H. & Savage, W. Z. 1989: Topographic and structural conditions in areas of gravitational spreading in the Western United States. *U.S. Geological Survey Professional Paper 1496,* 1-27.

Walder, J.S. & Hallet, B. 1985: A theoretical model of the fracture of rock during freezing. *Geological Society of America Bulletin 96,* 336-346.

Whitehouse, I. E. & Griffiths, G. A. 1983: Frequency and hazard of large rock avalanches in the central southern Alps, New Zealand. *Geology 11,* 331-334.

Wieczorek, G. F. & Jäger, S. 1996: Triggering mechanisms and depositional rates of postglacial slope-movement processes in the Yosemite Valley, California. *Geomorphology 15,* 17-31.

Wyrwoll, K-H. 1977: Causes of rock-slope failure in a cold area: Labrador-Ungava. *Geological Society of America Reviews in Engineering Geology 3,* 59-67.

Zischinsky, U. 1966: On the deformation of high slopes. *First Congress of the International Society of Rock Mechanics 2,* 179-185.

Zwaan, K. B. 1988: Bedrock map Nordreisa, M 1:250 000. Geological Survey of Norway.

Zwaan, K. B., Farseth, E. & Grogan, P. W. 1998: Bedrock map Tromsø, M 1:250 000. Geological Survey of Norway.